

János Haas

# Characteristics of peritidal facies and evidences for subaerial exposures in Dachstein-type cyclic platform carbonates in the Transdanubian Range, Hungary

Published online: 29 July 2004  
© Springer-Verlag 2004

**Abstract** In the Late Triassic, an extremely large carbonate platform system (Dachstein-type platforms) developed on the margin of the Neotethys. On the wide inner platform cyclic peritidal, lagoonal successions were deposited. In the Transdanubian Range (Hungary), the lower part of the 1.5–2-km-thick cyclic succession (Upper Tuvalian–mid-Norian) is pervasively dolomitised, the upper part (Upper Norian–Rhaetian) is non-dolomitised; there is a transitional interval between them made up of partially dolomitised cycles. The peritidal–lagoonal cycles are commonly bounded by well-developed disconformity surfaces reflecting subaerial erosion that punctuated the marine carbonate accumulation. Truncation of the cycles was preceded by pervasive cementation of the previously deposited cycle. In the early stage of the platform evolution, tidal flat dolomitisation under semi-arid conditions led to the consolidation of the previously deposited sediments. The truncation surfaces were commonly covered by dolocretes. During the more humid Late Norian–Rhaetian period, the early cementation was followed by karstification, accumulation of wind-blown dust and pedogenesis. Erosion during regularly recurring subaerial exposure that commonly reached the previously deposited subtidal beds suggests eustatic control of the cyclicity and supports the application of an allocyclic model, even if the Milankovitch signal is imperfect.

**Keywords** Upper Triassic · Transdanubian Range · Dachstein Formation · Carbonate platform · Peritidal facies · Sedimentary cycles · Carbonate diagenesis

## Introduction

In the Late Triassic, an extremely large carbonate platform system developed along the margins of the Neotethys Ocean (Fig. 1) that resulted in the accumulation of a huge volume of platform carbonates. In the Northern Calcareous Alps these platform carbonates have been studied since the 19th century (Simony 1847; Peters 1855; Gümbel 1857; Pia 1923; Sander 1936; Schwarzacher 1948, 1954; Fischer 1964; Zankl 1967; Piller 1976; Tollmann 1976, 1985; Fruth and Scherreiks 1984; Schwarzacher and

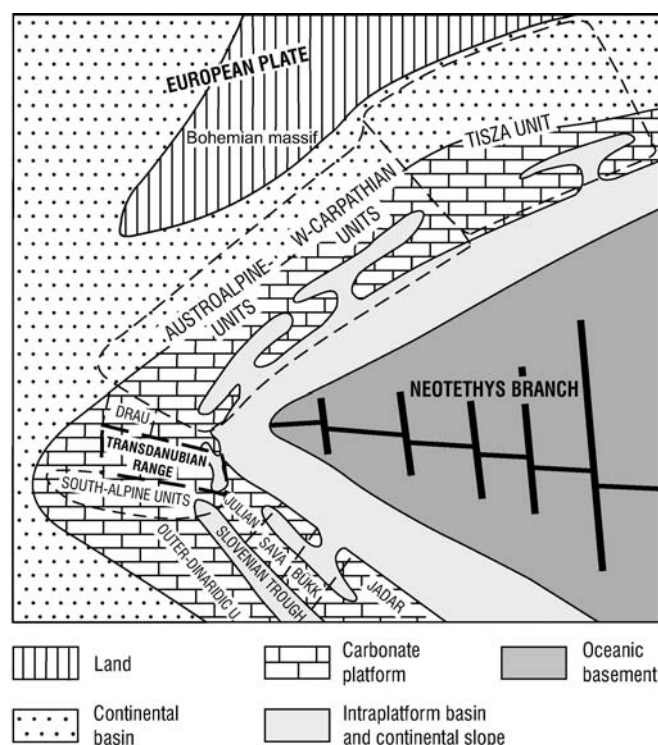


**Fig. 1** Paleogeographic reconstruction of the area at the western termination of the Neotethys Ocean in the Norian showing paleo-position of the Transdanubian Range

J. Haas (✉)  
Geological Research Group  
of the Hungarian Academy of Sciences,  
Eötvös Loránd University,  
Pázmány sétány 1/c, 1117 Budapest, Hungary  
e-mail: haas@ludens.elte.hu

Haas 1986; Haas et al. 1995; Satterley and Brandner 1995; Satterley 1996; Enos and Samankassou 1998, 2002; Gawlick et al. 1999; Gawlick 2000; Mandl 2000). The platform limestone deposits were named the Dachstein Limestone while the dolomite was referred to as Dachstein Dolomite or Hauptdolomit. Thick Upper Triassic (Upper Tuvallian–Rhaetian) platform carbonate sequences with features akin to those in the type locality of the Dachstein Limestone and Dachstein Dolomite in the Eastern Alps occur in the Central and Inner Western Carpathians (Michalik 1980, 1993), Southern Alps (Bossellini 1967; Bossellini and Hardie 1988; Jadoul et al. 1992; Ogorelec and Rothe 1992; Iannace and Frisia 1994; Ogorelec and Buser 1996; Cozzi et al. 2003), Dinarides (Dimitrijevic and Dimitrijevic 1982, 1991), Hellenides (Pomoni-Papaioannou et al. 1986; Haas and Skourtsis-Coroneou 1995); and also in the northern part of the Pannonian Basin (Végh-Neubrant 1957, 1960; Oravecz 1963; Fülöp 1976; Haas 1982; Gecse 1984; Schwarzscher and Haas 1986; Haas 1991, 1994; Haas et al. 1995; Haas and Balog 1995; Haas and Budai 1995; Balog et al. 1997, 1999; Mindszenty and Deák 1999; Haas and Demény 2002). Although the formal lithostratigraphic names of these formations differ regionally, one can refer them collectively as Dachstein-type platform carbonates.

In the Transdanubian Range (Hungary) the Dachstein-type platform carbonates developed with a remarkable areal extension and thickness. The lack of metamorphism and only moderate tectonics provide an excellent opportunity for studying the original facies relationships and depositional structures, especially where the cyclic inner platform successions are concerned.

The cyclic nature of the Dachstein Limestone was initially recognised by Sander (1936) and Schwarzscher (1948). However, Fischer (1964) was the first to propose a peritidal origin of those distinctive layers that regularly punctuate the subtidal lagoonal carbonate succession.

In the last decades, two basic models were proposed to explain the observed cyclic pattern: allocyclic (Fischer 1964, 1975, 1991; Haas 1982, 1991, 1994; Schwarzscher and Haas 1986; Balog et al. 1997; Cozzi et al. 2003) and autocyclic (Satterley and Brandner 1995; Satterley 1996; Enos and Samankassou 1998, 2002). According to the allocyclic model, orbitally forced sea-level oscillation controlled the formation of the Lofer cycles. The autocyclic model (Ginsburg 1971) involves progradation of tidal flats as a result of landward movement of the carbonate sediment from the subtidal carbonate factory. Expansion of the tidal flats reduces the area of the subtidal carbonate factory, leading to sediment starvation, gradual decrease of sedimentation rate, and finally an end to progradation. Subsidence of the basement leads to resumed subtidal conditions and gives rise to the re-establishment of the carbonate factory. Shallowing-upward cycles consisting of subtidal–peritidal couplets may form in this way.

The main target of this paper is to present the results of detailed studies of the cycle-bounding erosion surfaces and the related peritidal facies. This approach may help

decide whether the allocyclic model or the autocyclic one is more appropriate for sedimentation of Dachstein-type platform carbonates. Because very thin, commonly argillaceous layers, and subtle karstic features, which are barely visible even in the best natural outcrops, are the focus of this study, the availability of large quarries in the Transdanubian Range, and of cores that include significant parts of the Dachstein-type platform carbonates was of crucial importance.

## Geological setting

The Dachstein-type platform carbonates are intermittently exposed in the Transdanubian Range (TR) over a distance of 270 km (Fig. 2). The NE–SW strike of the mountain range is roughly perpendicular to the trend of the facies belts. The thickness of the platform carbonates is 1.5–2 km. The platform–carbonate complex can be subdivided into several lithostratigraphic units (Fig. 3). These units reflect differences in sedimentological and early diagenetic conditions that were controlled by the paleogeographic setting as well as by tectonic, eustatic and climatic factors. All of these controlling factors underwent changes during the history of platform that spanned approximately 16 million years. Chronostratigraphy of the Dachstein-type platform carbonates is based mainly on the Megalodontaceae fauna (Végh-Neubrant 1982) and the locally rich foraminifera assemblage (Oravecz-Scheffer 1987). These fossils allow subdivision at the stage and locally at the substage level. However, ammonite and conodont-bearing basin facies that occur below and above the platform carbonates and may also interfinger with them (see Fig. 3), provide additional tools for chronostratigraphy (Haas 2002).

In its early stage, in the Late Tuvallian–Late Norian, unidirectional facies polarity characterised the paleogeographic setting. The north-eastern part of the TR represented the seaward margin of an attached platform where intraplatform basins were developed roughly parallel to the platform margin as a result of the Neotethys rifting (Haas et al. 1995; Gawlick et al. 1999). Deposition of oncoidal limestone with patch reefs (oncoidal Dachstein Limestone) characterised the outer platform belt (Haas and Budai 1995). In the inner platform, accretion of a cyclic peritidal and lagoonal carbonate succession took place in part coevally. The inner platform was affected by pervasive early diagenetic dolomitisation under the prevailing semi-arid climate to produce the Földolomit Formation (Hauptdolomit, Dachstein Dolomit or Dolomia Principale). More humid climatic conditions in the mid-Norian led to partial, i.e. formation of the Fenyőfő Member of the Dachstein Limestone, which is actually a transitional unit between the Földolomit and the Dachstein Limestone. In the Late Norian, significant changes took place in the paleogeographic setting. As a consequence of the incipient rifting of the Ligurian–Penninic Ocean branch, extensional basins were developed in the south-western part of the TR (Kössen-type basins). The attached

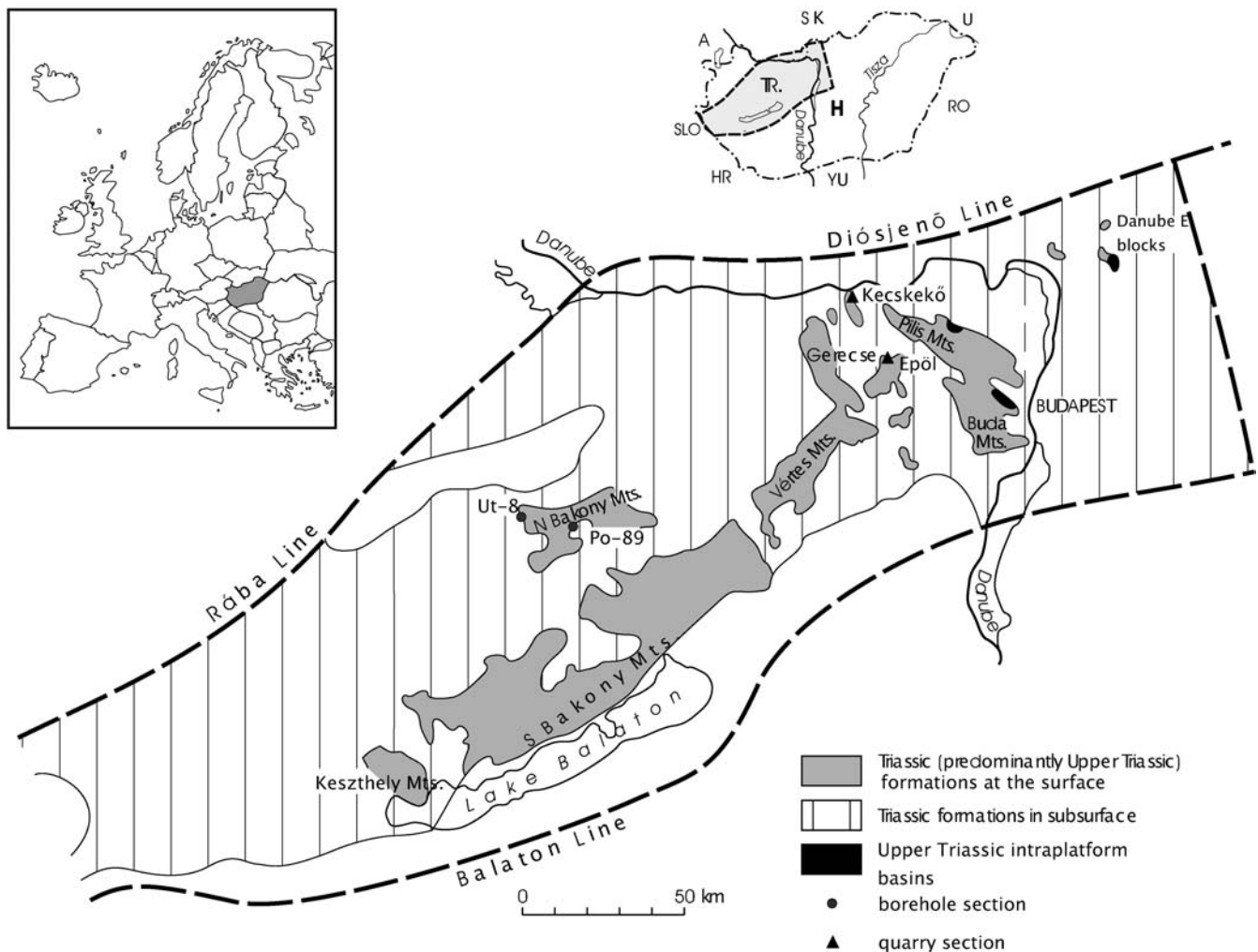


Fig. 2 Triassic formations in the Transdanubian Range and location of the sections studied

platform was transformed into an isolated platform, leading to a double facies polarity in the latest Norian (Haas 2002). The trend of increasing humidity continued, leading to cessation of early diagenetic dolomitisation on the platform and consequently onset of development of Dachstein Limestone, whereas formation of lagoonal dolomite was followed by accumulation of fine siliciclastics in the coeval Kössen-type basins (Haas and Budai 1995).

The Upper Triassic inner platform successions in the TR are characterised by Lofer-type cycles. For the Dachstein Limestone in the TR the mean cycle thickness is 3.1 m (Schwarzacher and Haas 1986; Haas 1991). The mean thickness of the basic cycles in the transitional Fenyőfő Member and in the Fődolomit Formation is practically the same. The basic facies types and sequences within the cycles are similar in each lithofacies unit, although there are remarkable differences in the relative abundance of the cycle-types (Fig. 4) and in the relative thickness of the members within individual cycles. There is no significant difference among the lithofacies units in terms of the facies characteristics of the subtidal beds. In

contrast, the peritidal deposits and those features that were formed under subaerial conditions are markedly different.

### Cyclicity and effects of subaerial exposures

#### Dolomitised successions

In the Fődolomit Formation, 800–1200 m thick, the cycles typically consist of two basic rock types: microbial stromatolite (Member B, using Fischer's subdivisions) and various subtidal facies (Fischer's Member C), including bioclastic, ooidic and peloidal wackestone or packstone and crystalline dolostone without any recognisable depositional texture. The cycles are generally bounded by irregular disconformity surfaces (d). Red, argillaceous and commonly laminated, brecciated and rarely pisoidic dolomite (dolocrete; Balog et al. 1997), a few cm in thickness, may occur above the disconformity. The cycle-bounding disconformity may be either below the stromatolitic member or above it, or in many cases it is within



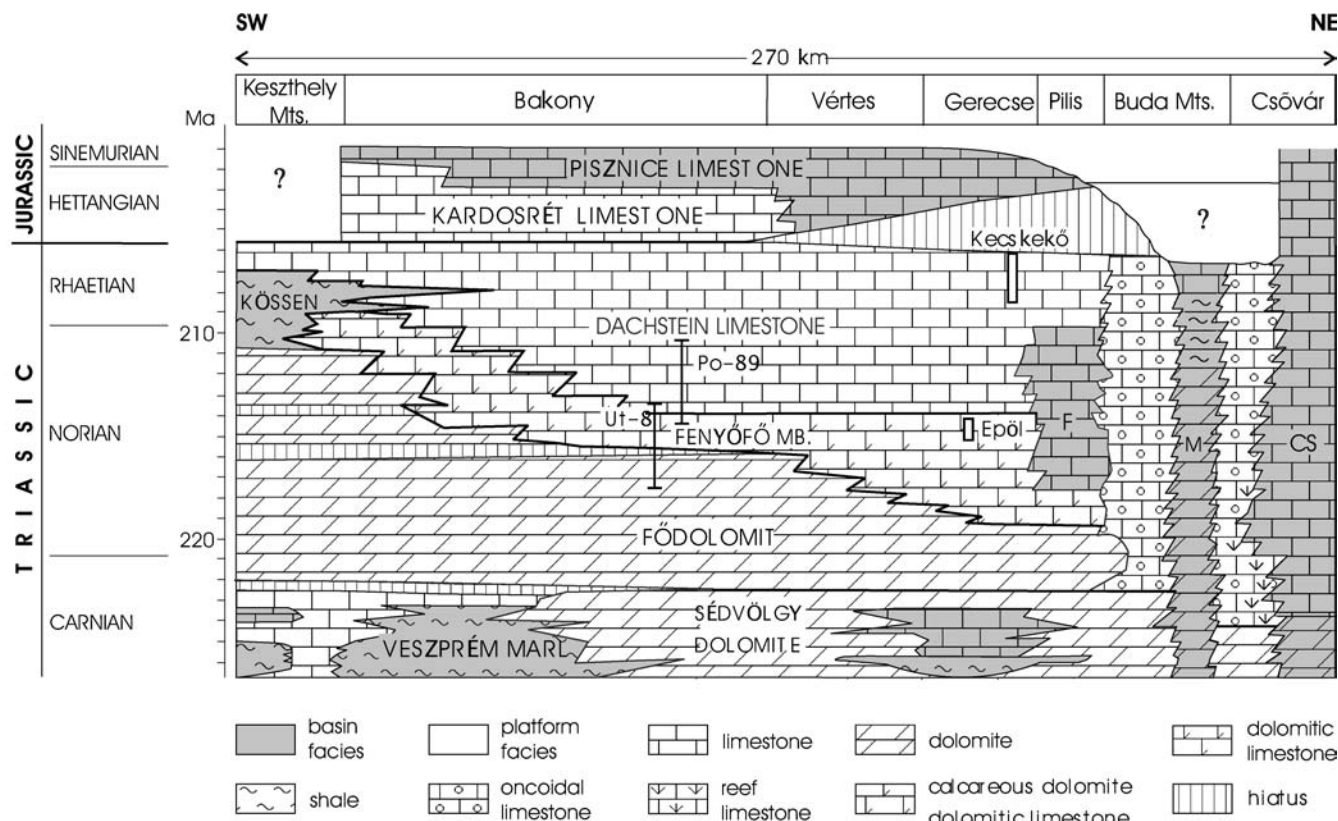


**Fig. 3** Stratigraphic chart for the Upper Triassic of the Transdanubian Range and stratigraphic setting of the sections studied (modified after Haas 2002; timescale: Gradstein and Ogg 1996).

For locations see Fig. 2. Abbreviations: *F* Feketehegy Formation, *M* Mátyáshegy Formation, *CS* Csővár Formation

the stromatolitic facies separating the regressive (B') and the transgressive (B) peritidal members (see Fig. 4). This means that the ideal cycle pattern is d-B-C-B'-d, although truncated cycles (d-B-C-d) are common. Rhythmic alternations of peritidal and subtidal facies without any bounding erosional surface (B-C-B-C) was also observed in some intervals.

For the evaluation of the conditions of subaerial exposure, three aspects are crucial including (1) the existence of truncated cycles, e.g. the regressive peritidal facies are commonly missing, so the C member is bounded upward by a disconformity; (2) the occurrence of dolomite caps, appear to be best developed under semi-arid or seasonally wet-dry climatic conditions in the subaerial period (James 1972; Read 1974; Wright and Tucker 1991); and (3) early diagenetic pervasive dolomitisation that took place beneath the surface of the tidal flat in the unconsolidated mud. According to the C and O isotope composition of these dolomite types, slightly concentrated sea water may have been the dolomitising fluid (Balog et al. 1999).

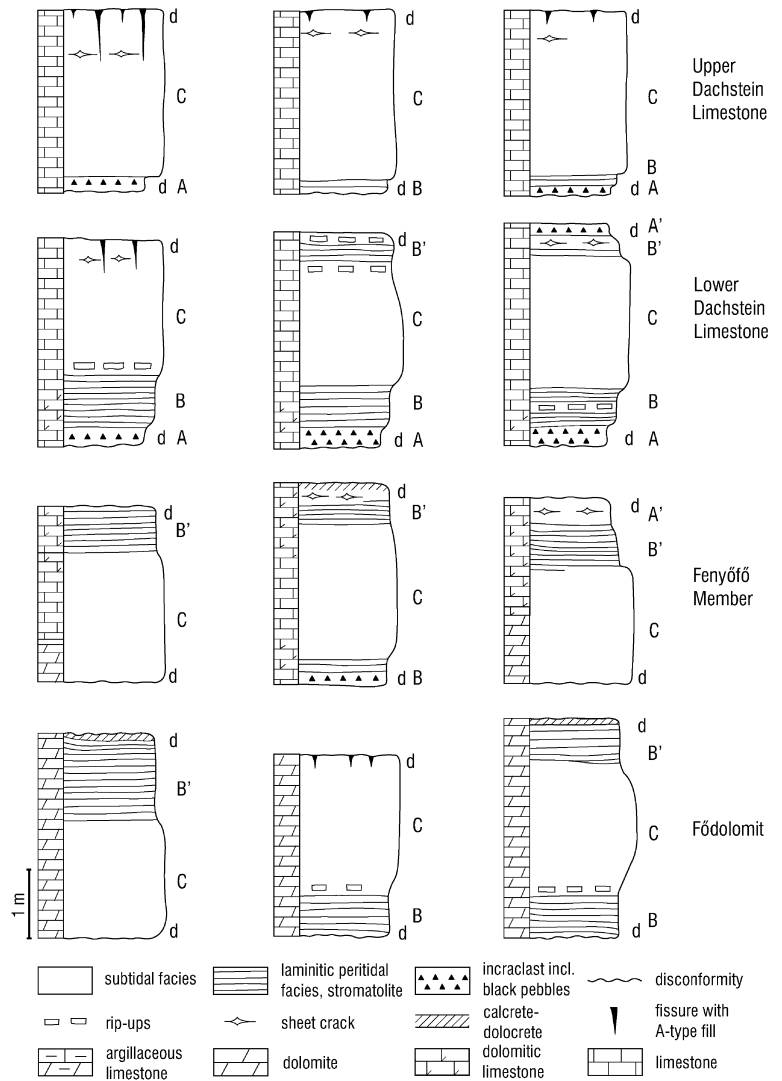
The Fenyőfő Member forms a transitional interval, 100–300 m-thick between the Földolomit Formation and the typical Dachstein Limestone. It is characterised by calcareous dolostone and dolomitic limestone, and by alternation of dolomitised and non-dolomitised intervals. A complete succession of the Fenyőfő Member was re-

covered in core Ugod Ut-8 in the Northern Bakony. The upper part of the member was recovered in core Porva Po-89, in the Northern Bakony, and it is exposed in the Epöl quarry, in the Gerecse Mts. (for locations see Figs. 2 and 3).

The dolomitisation is more pronounced in the lower part of the member where characteristics of the cycles are similar to those in the Földolomit Formation. There is a definite upward decrease in the extent of dolomitisation. Decreased dolomitisation is accompanied by a general increase in reddish or greenish argillaceous, commonly intraclastic facies above the disconformity at the base of the cycles (Fischer's Member A) (Fig. 4). Thus, the cycle pattern typical in the lower part of the Dachstein Limestone (d-A-B-C-B'-d) appears gradually. According to petrologic and stable-isotope studies (Haas and Demény 2002), dolomitisation took place in the unconsolidated sediments of the previously deposited cycle through downward percolation and seaward flow of the slightly concentrated sea water. Mixing of sea water and meteoric water may have also played a role in this process.

As in the case of the Földolomit Formation, the most important subaerial process is the dolomitisation itself. The dolomitisation occurred mainly from evaporated sea water generated on the repeatedly flooded tidal flat. Karstification and accumulation of the reworked argilla-

**Fig. 4** Characteristic facies sequences of the elementary cycles in the Upper Triassic carbonate successions in the Transdanubian Range. Relative frequency of the cycle types decrease left to right. Abbreviations (using symbols of Fischer 1964 and Haas 1991): *d* disconformity, *A* red or green argillaceous, intraclastic carbonate at the base of the cycle, *A'* red or green argillaceous, intraclastic carbonate at the top of the cycle (below the main disconformity surface), *B* microbial stromatolite at the lower part of the cycle, *B'* microbial stromatolite at the upper part of the cycle, *C* grey wackestone with shallow marine biota



ceous weathering products show an inverse relation to the intensity of the early dolomitisation.

#### Non-dolomitised successions

In the TR, the Dachstein Limestone s. str. is 600–900 m thick and can be subdivided into two parts based on characteristics of the Lofer cycles. The lower part corresponds approximately to the Middle–Upper Norian while the upper part corresponds roughly to the Rhaetian.

#### Lower Dachstein Limestone (Norian)

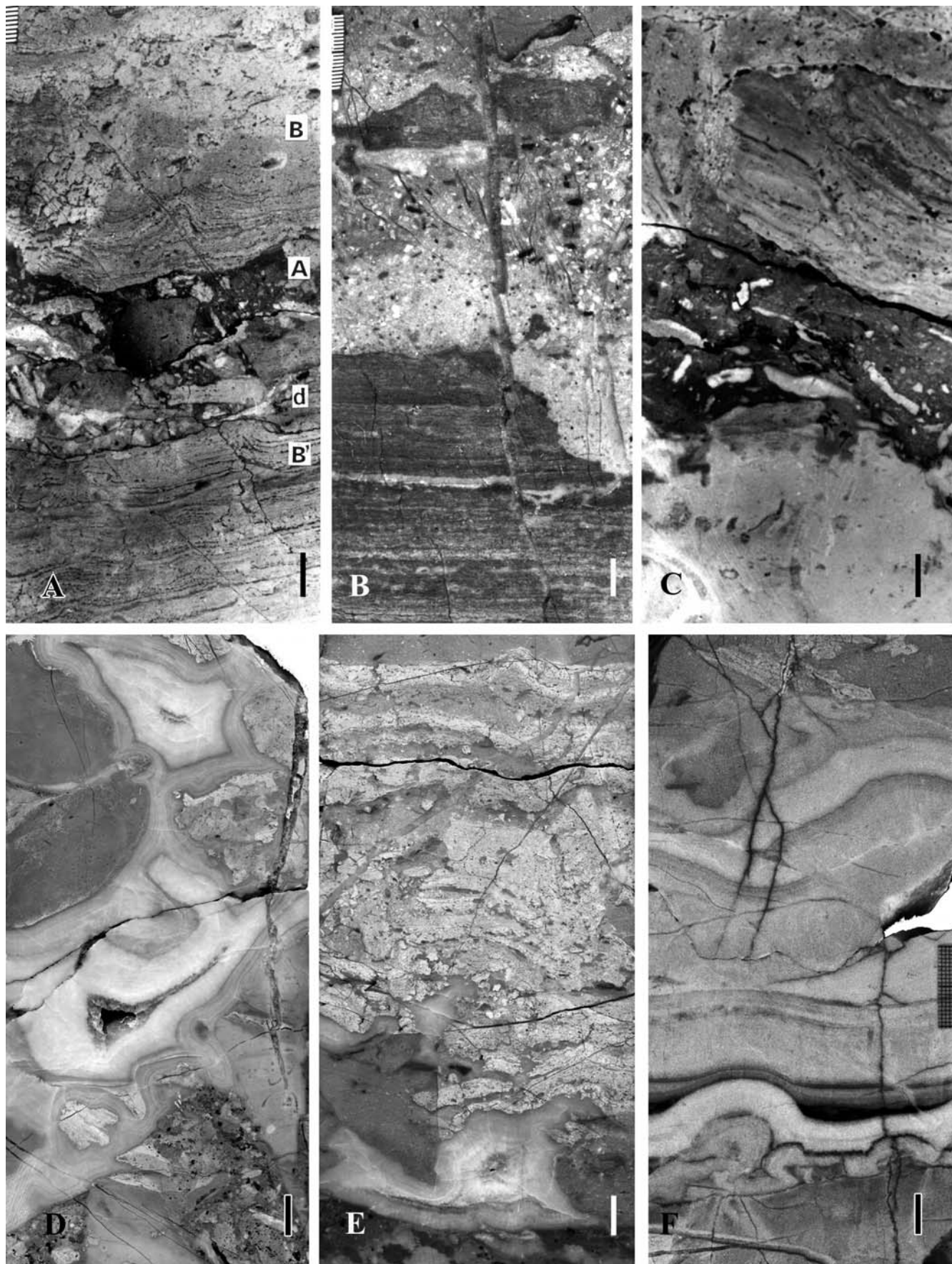
Above the transitional Fenyőfő Member, the lower part of the Dachstein Limestone s. str. approximately 500–700 m thick, is generally made up of fairly complete and symmetrical cycles (*d*-*A*-*B*-*C*-*B'*-*A'*-*d*), although truncated ones (*d*-*A*-*B*-*C*-*B'*-*d* or *d*-*A*-*B*-*C*-*d*) are also common (see Figs. 4 and 5A, B). The disconformity surfaces (*d*) are generally irregular, showing traces of karstic solution

(Fig. 5C). Solution pockets and cavities (5–10 cm in size) that are filled by reddish or greenish argillaceous limestone are common. Metre-scale karstic cavities and fractures also occur, although rarely.

#### Facies analysis of selected parts of the studied section

In accordance with the main goals of this paper, the best core of the lower part of the Dachstein Limestone was selected for detailed investigation of the peritidal deposits and evidence for subaerial exposure. The Porva Po-89 core was cut in the central part of the Northern Bakony Mts. It recovered a continuous 400-m succession of the Dachstein Limestone from the upper part of the Fenyőfő Member that was not affected by any appreciable tectonic disturbance. The recovered interval can be classed as Norian, based on the Megalodontaceae fauna and the Foraminifera assemblage (Haas 1995a). The succession is made up of cyclic alternation of peritidal and subtidal beds as is shown on Fig. 6. Basic facies characteristics (both macrofacies and microfacies) of the cycle members





have been described earlier (Haas 1982; Balog et al. 1997). A more detailed investigation of facies characteristics and early diagenetic alterations of the layers between the subtidal beds are the focus of the present study in order to determine the mode of superposition of the cycles, continuity vs. discontinuity. Intervals studied in detail are indicated on Fig. 6.

Results of the studies on the selected core sections and interpretation of the observations are summarised in Figs. 7, 8, 9, 10, 11 and 12. These figures show the basic lithology, rock colour, macrofacies and microfacies types, basic characteristics of the intraclasts, and the type of porosity together with features of pore filling. In some cases, interpretation of the depositional history of the section studied is also displayed (Figs. 9, 11, 12B), assuming that the basic cycles represent equal rates.

### *Peritidal facies and genetic interpretations*

Based on studies of the Dachstein Limestone in the classic sections of the Northern Calcareous Alps, Fischer (1964) defined “conglomerate with red or green matrix” (p 113) at the base of the Lofer cycle as Member A. He also noted that Member A is generally argillaceous, pelletal, locally ostracode-bearing, and commonly occurs as internal sediment in cavities, sheet cracks and fissures. Fischer interpreted this facies as “modified and redeposited soil” of “local origin” that was formed “mainly by solution along the disconformity” (p 123).

Fischer (1964) suggested the term “loferite” for “limestones and dolomites which are riddled by shrinkage pores” (p 124). He defined Member B as “loferites with algal mats and abundant desiccation features” (p 113) and interpreted as intertidal facies. Four main types of lofer-

**Fig. 5** Erosional cycle boundaries and solution cavities. **A** Boundary of two cycles. **B'** Microbial stromatolite in the topmost part of the underlying cycle, *d* disconformity surface, *A* red, intraclastic argillaceous micrite containing mm- to cm-sized clasts showing features of *A* and *B* facies types. Core Po-89, 411.0–411.2 m. Scale bar is 1 cm. **B** Erosional surface indicating truncation of a microbial stromatolite (*B'*) member. It is overlain by red, intraclastic argillaceous micrite containing small white, grey, and black intraclasts and larger rip-ups of microbial stromatolite. Core Po-89, 163.4–163.7 m. Scale bar is 1 cm. **C** Subtidal facies with megalodonts (*C* member) is visible in the lower part of the photo. It is truncated by an irregular (microkarstic) disconformity surface that is covered by intraclastic argillaceous micrite (*A* member) representing the base of the overlying cycle. The *A* member is overlain by intraclastic limestone containing a large rip-up of microbial stromatolite and small black intraclasts. Po-89, 360.4–360.6 m. Scale bar is 1 cm. **D** Solution cavities that were filled with generations of isopachous calcite cement under marine phreatic conditions and subsequently with drusy calcite probably of meteoric origin in the central part of the pores. Po-89, 159.8–160.0 m. Scale bar is 1 cm. **E** Solution cavities in brecciated stromatolite. The cavity in the lower part of the photo is filled by isopachous calcite cement, micritic internal sediment, and drusy calcite. Po-89, 127.3–127.5 m. Scale bar is 1 cm. **F** Lens-shaped, bedding-parallel solution cavities filled by isopachous calcite cement. Po-89, 127.3–127.5 m. Scale bar is 1 cm

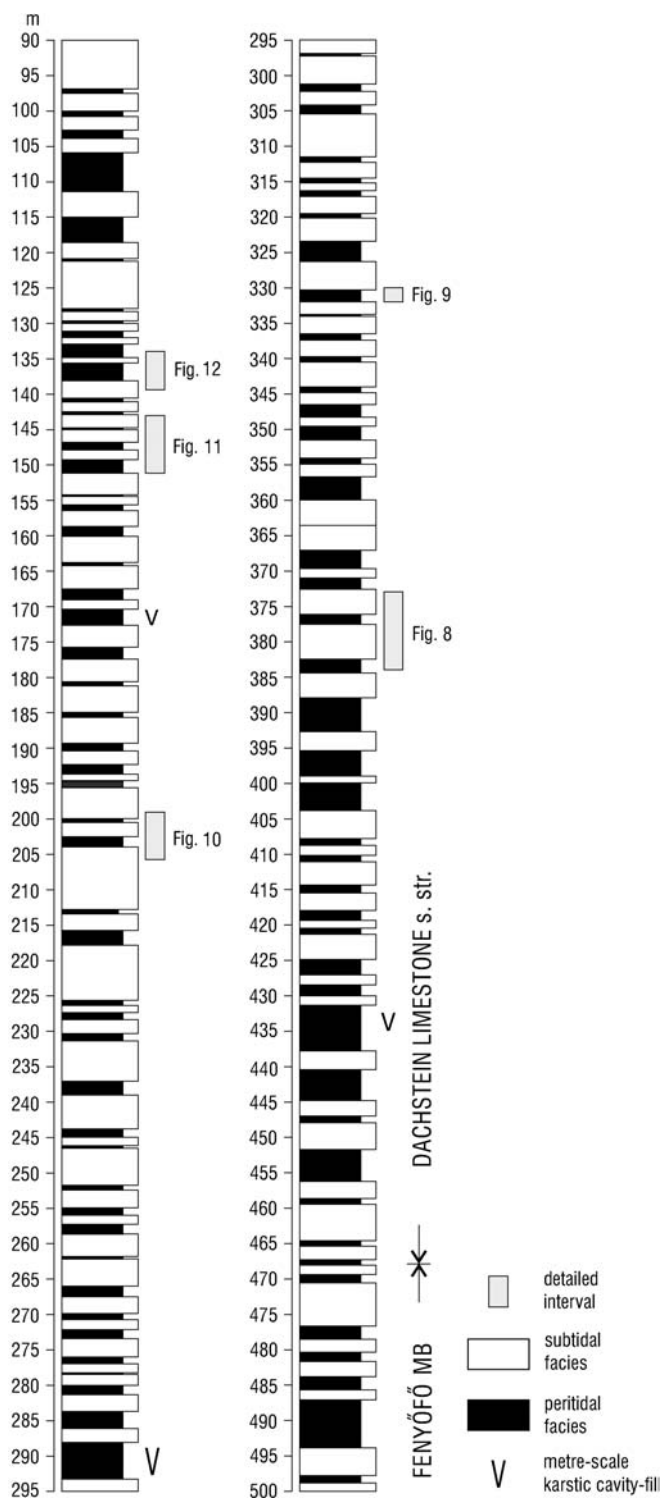


**Fig. 6** Cyclic alternation of the peritidal and subtidal facies in the core Po-89, Bakony Mts., which recovered a 400-m-thick interval of the lower (Norian) part of the Dachstein Limestone

ites were distinguished “algal mat, pellet, homogeneous and conglomeratic” (p 127).

In the studied section in the TR, between the subtidal beds of predominantly skeletal and peloidal wackestone or packstone, facies types akin to those that were de-



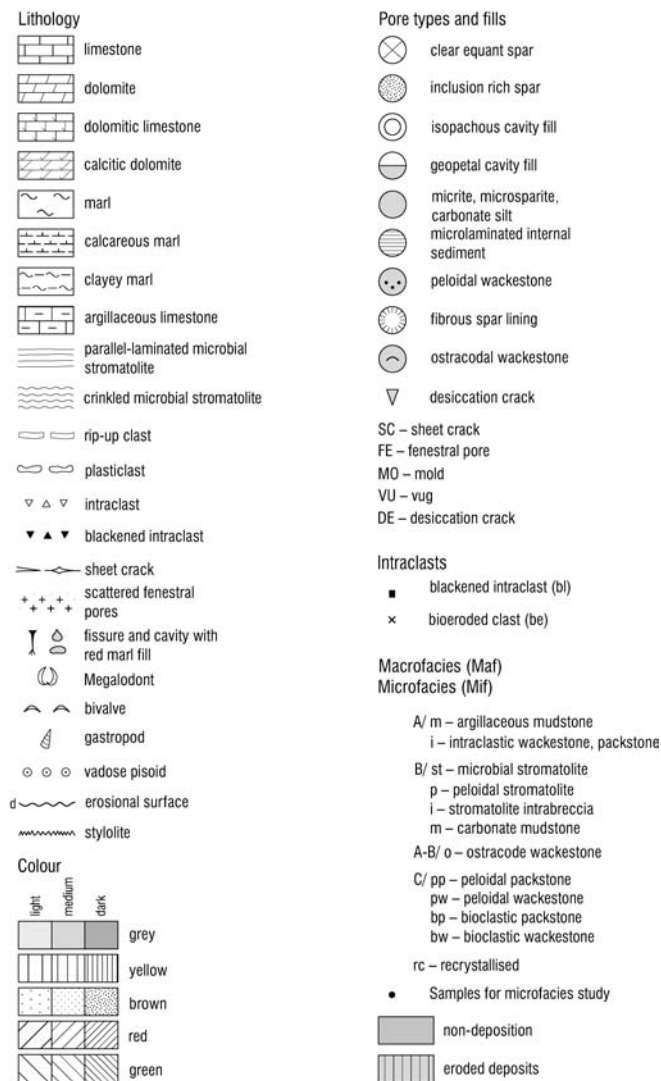


Fig. 7 Legend to Fig. 8, Fig. 9, Fig. 10, Fig. 11, Fig. 12

scribed by Fischer as A and B members were found. Description and genetic interpretation of the distinguished facies types are summarised below. Genetic interpretation is based mainly on investigations of modern tidal flat carbonate environments (Ginsburg and Hardie 1975; Shinn 1983; Hardie and Shinn 1986; Foos 1991; Wright 1994).

#### Member A:

1. Argillaceous micrite, carbonate silt (dolosilt), clayey marl or marl, greenish or reddish (code on the figures: A/m). Scattered fenestral pores with geopetal fills may occur.

Interpretation: tidal-flat deposit forming after a prolonged subaerial exposure period. It is a mixture of marine carbonate mud and probably airborne fine siliciclastics and/or carbonates (Foos 1991; Wright 1994) that were not or only slightly affected by pedogenesis following the last deposition.

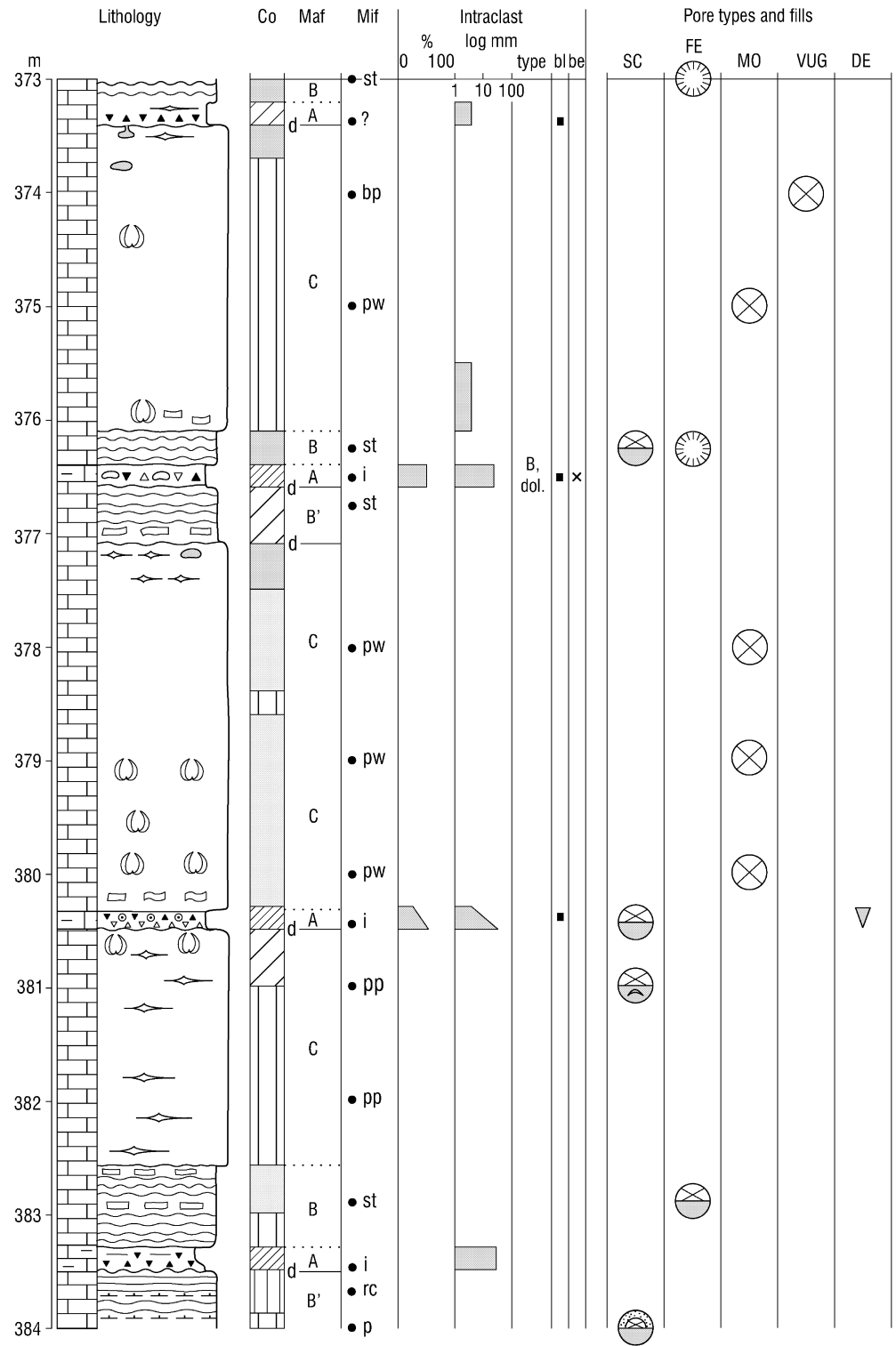
2. Intraclastic argillaceous micrite, greenish or reddish, rarely with silt-sized quartz and mica (A/i). The most characteristic of the millimetre- to centimetre-sized intraclasts are rip-ups of microbial stromatolite (Fig. 14A, B), blackened pebbles (Fig. 14C), red pisoids, pisoidic lumps and aggregates with Fe-oxide staining, cement and coating (Fig. 14D, E). Ostracodes are usually common in the matrix. In a few cases, thin carbonate pisolite interlayers were found in this facies. Interpretation: tidal flat—tidal channel lag-deposit forming after a prolonged subaerial exposure period. Ostracodal matrix of the intraclastic facies constrains subaqueous depositional environment. The composition of the pebbles provides valuable information on the ambient penecontemporaneous environments. Most probably staining by terrestrial organic matter caused the blackening of a number carbonate pebbles (Strasser and Davaud 1983; Strasser 1984; Vera and Jiménez de Cisneros 1993). Red coated grains and aggregates with Fe-oxide staining and cement are probably of pedogenic origin (Foos 1991; Wright 1994). It means that subaerial conditions prevailed prior to, and/or penecontemporaneous with, the onset of the tidal-flat deposition. The carbonate pisoids were probably formed in supratidal or intertidal pools (Wright 1994).

#### Member B:

1. Microbial stromatolite, light grey, yellowish, pinkish, with fenestral pores, (B/st). The laminations are planar or wrinkled (Fig. 15A, B, C, E). In a few cases calcified cyanobacteria (?) filaments are preserved (Fig. 15F). Interpretation: tidal flat—interchannel intertidal and supratidal area that was covered by a microbial mat. Crinkly lamination with fenestral pores indicates intermittent exposure and desiccation (Riding 1991). Preservation of fenestral pores via early diagenetic cementation suggests supratidal environment (Shinn 1983). Calcification of cyanobacteria filaments is typical in freshwater marsh environments and does not take place in areas frequently inundated by seawater (Monty and Hardie 1976; Tucker 1990).
2. Peloidal microbial stromatolite (Fig. 15D), akin to the previously described type, but with large amounts of tiny peloids (B/p). Interpretation: tidal flat—interchannel intertidal and supratidal area that was covered by a microbial mat. The peloids are either trapped sedimentary particles (agglutinated stromatolites; Riding 1991) or calcified microbes (Friedman et al. 1973).
3. Stromatolite intra-breccia (B/i). In the majority of cases the millimetre to centimetre-sized rip-up clasts of stromatolite appear directly above the basal stromatolite layer in a mudstone or wackestone matrix (Fig. 16B,D). Both clast and matrix-supported breccia occur. Larger rip-ups of stromatolite occasionally with small blackened intraclasts may also occur near to the



**Fig. 8** Lithology, macrofacies and microfacies types, intra-clasts, pores and pore filling in the 373–384-m interval of core Po 89, Bakony Mts.



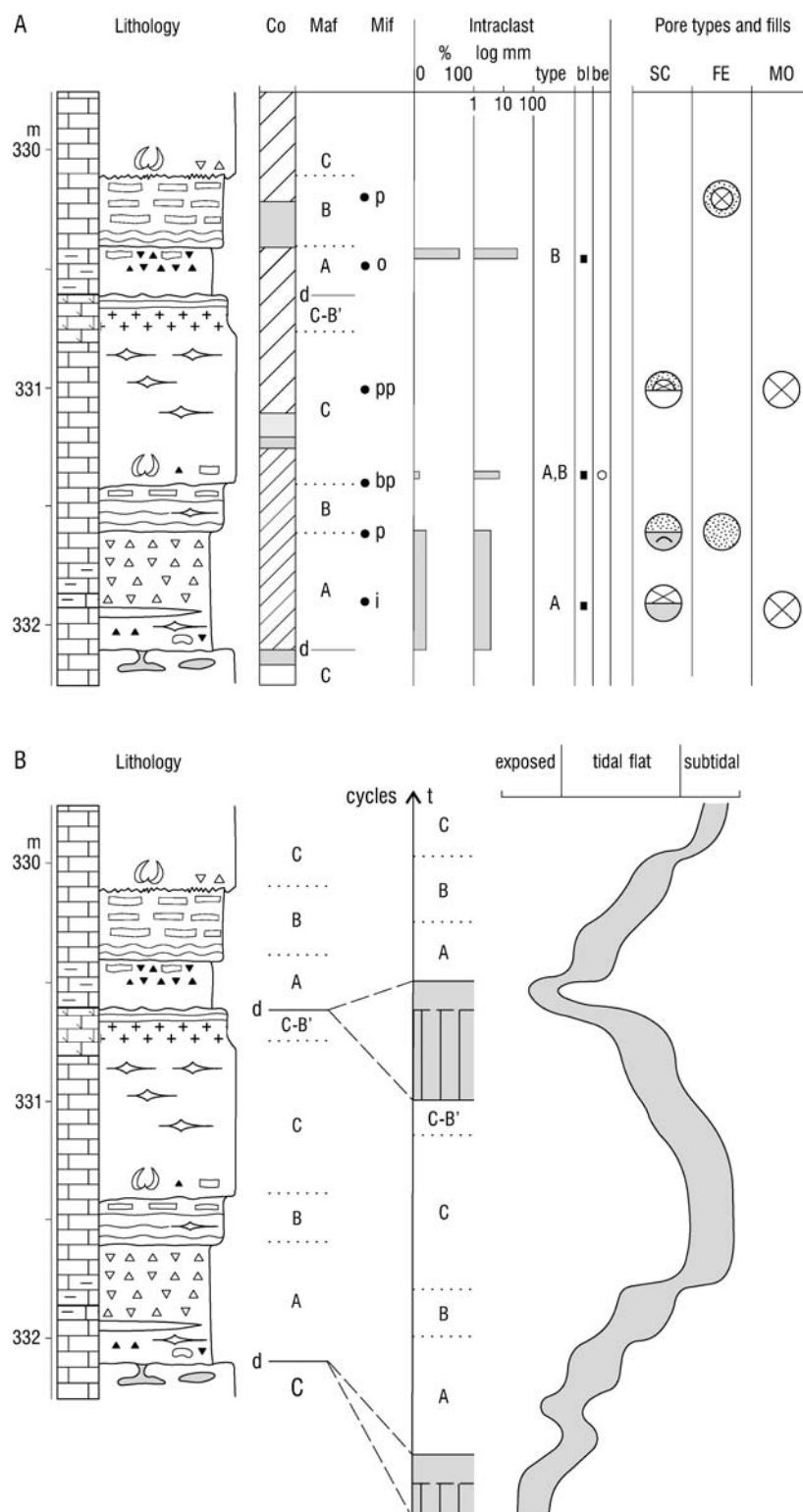
base of the cycles (Fig. 15G). In-situ incipient brecciation of microbial stromatolite could also be observed (Fig. 16A).

Interpretation: tidal flat—supratidal area. Such intra-clasts are typically formed by desiccation of the microbial mat followed by erosion and redeposition, mainly by storms (Shinn 1983). Burrowing also results in the disruption of stromatolites, but rarely.

4. Mudstone, light grey, yellowish, or pinkish, with scattered fenestral pores (B/m).

Interpretation: tidal flat—supratidal area. Preservation of fenestral pores in fine carbonate mud implies active early diagenetic cementation that is common in the supratidal zone (Shinn 1983).

**Fig. 9** **A** Lithology, macrofacies and microfacies types, intraclasts, pores and pore filling and **B** interpretation of the paleoenvironment in the 330—332-m interval of core Po-89, Bakony Mts.



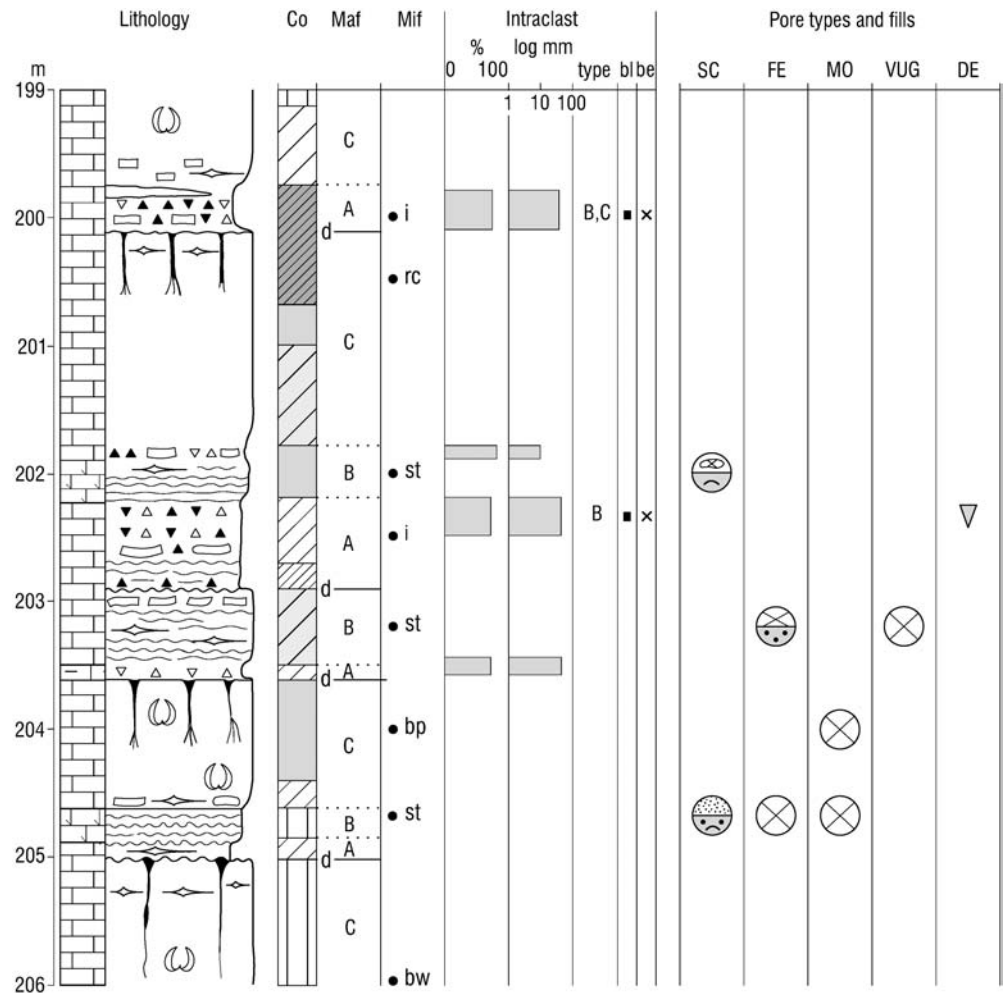
#### Member A and B:

1. Ostracode wackestone, reddish, greenish or light grey (A-B/o). It may be in close association either with facies type No. 1 (A/m) or No. 6 (B/m), and this facies is the most common pore and cavity fill. Thin-walled

ostracodes are typical. Preserved double valves are common (Fig. 16C, E, F). Out of ostracodes no other fossils typically occur in this facies.

Interpretation: tidal-flat pond deposit. Common occurrence of double-valved ostracodes suggests practically

**Fig. 10** Lithology, macrofacies and microfacies types, intra-clasts, pores and pore filling in the 199–206-m interval of core Po-89, Bakony Mts.



in-situ deposition, long-distance post-mortem transportation is highly improbable. It means that tidal-flat ponds may have been the habitat of the ostracode assemblage. A special ostracode biofacies consisting of halo-tolerant forms was reported by Benson (1959) in modern salt-water lagoon and marsh environments in Todos Santos Bay Region, Baja, California, Mexico. An ostracode assemblage of similar ecologic properties may have inhabited the tidal-flat ponds of the Dachstein-type platform.

All of the facies types described above were formed on the tidal flat, representing various subenvironments (channel, intrachannel intertidal and supratidal area, pond). No in-situ paleosol was found in the intervals studied, but in the reddish or greenish, typically argillaceous layers that frequently overlie the disconformity surface (Member A), redeposited remnants of subaerially modified and pedogenic deposits are common.

#### *Diagenetic features and their interpretation*

Many features of the Dachstein Limestone indicate intensive early lithification of the subtidal and peritidal

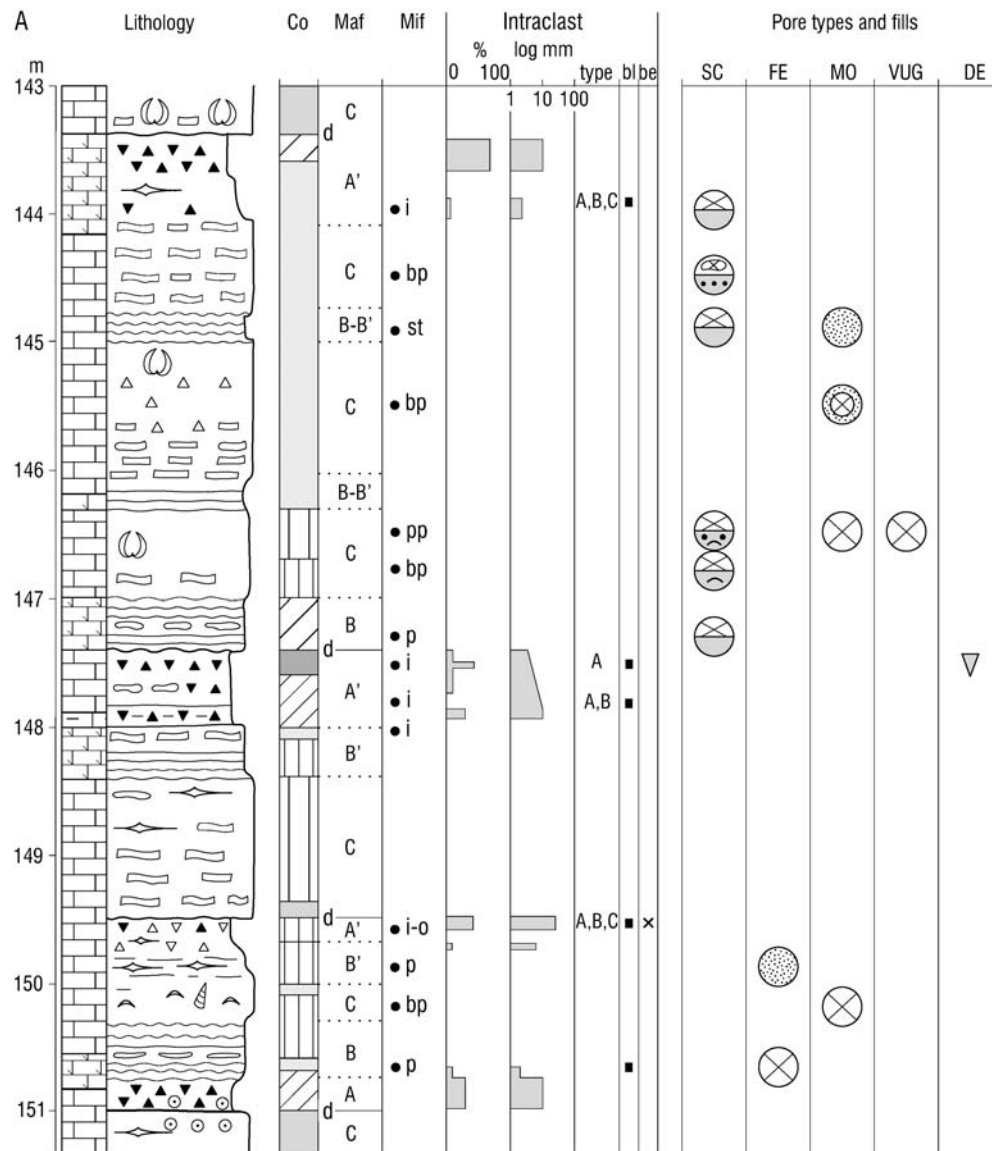
sediments, during a subaerial exposure interval subsequent to deposition of an individual cycle. The early lithification is evidenced by truncation of larger mollusc biomolds (generally megalodonts), traces of the karstic solution (Fig. 5C), and preservation of the fenestral pores, desiccation cracks, sheet cracks, gas blisters etc. The most common pore types are displayed in Figs. 8, 9, 10, 11, 12. The most important characteristics of the pore-filling material are also indicated.

In the peritidal layers desiccation cracks and sheet cracks are common. Cm-sized, irregular lens-shaped cavities with sparry calcite cement (gas blisters; Fischer 1964) also occur.

Solution pores ranging from millimetre to decimetre scale are common both in the peritidal and the subtidal beds, usually in the upper part of the cycles. Most are within half a metre of the cycle-bounding disconformity but some occur much deeper. The majority of the cavities are lens-shaped (Fig. 5F, G). They were probably formed at fossil water tables (Choquette and James 1988) suggesting the paleosurface a few decimetres to metres above the actual water table, which is in harmony with Read and Horbury's (1993) hydrologic model for humid tidal-flats.



**Fig. 11 A** Lithology, macrofacies and microfacies types, intraclasts, pores and pore filling and **B** interpretation of the paleoenvironment in the 143–151-m interval of core Po-89, Bakony Mts.



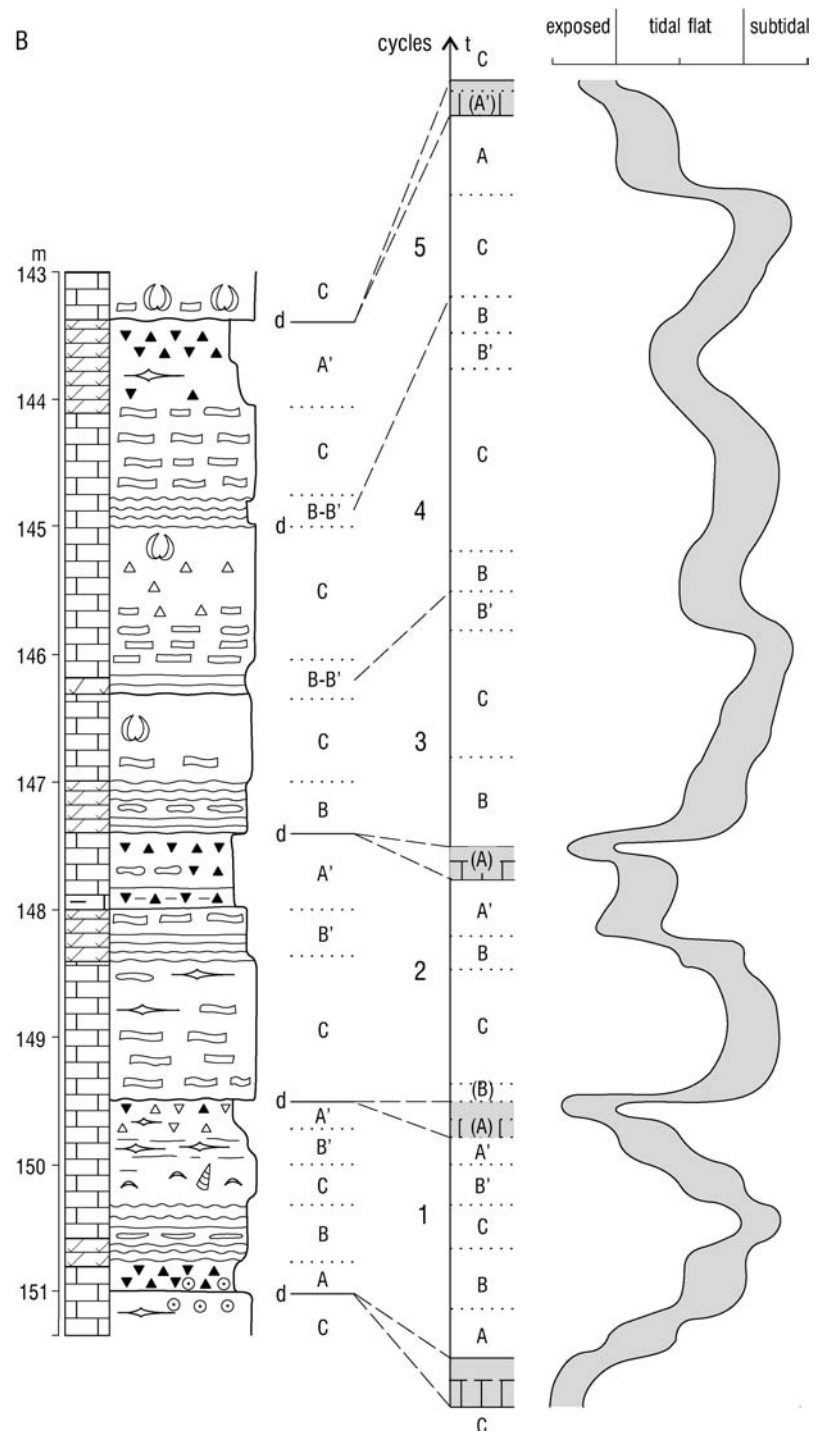
The isopachous calcite cement lining in the cavities was precipitated under phreatic conditions. In a lot of cases, fibrous isopachous lining, probably marine phreatic cement, covers the wall of the cavity, whereas coarse equant cement, probably of meteoric origin occur in the central part of the cavity (Fig. 5E).

The fenestral pores, sheet cracks and karstic solution pores are filled with internal sediments and sparry cement (Fig. 15B, D). Geopetal structures are common, with ostracode mudstone or wackestone filling the basal part of the voids (Fig. 16C, E). The surface of the basal intrasediment layer and the wall of the void are lined with inclusion-rich equant calcite spar, probably of marine origin. The internal part of the pore is filled with transparent sparry calcite. According to the stable isotope studies the isotopic composition of the calcite cement does not differ significantly from that of the coeval subtidal limestone and the assumed composition of the Tri-

assic sea water (Balog et al. 1999), suggesting a predominance of marine cementation.

Within peritidal environments there is a very close connection between sediment deposition and early diagenesis. Cyclic sediment deposition of the Dachstein-type platform carbonates led to cyclic early diagenesis. Lithification began with desiccation of the topmost mud layer when peritidal conditions were established. With more extended subaerial exposure, intense cementation and in-situ alteration of the previously deposited carbonate sediments took place. This was accompanied by karstic solution and bioerosion of the more or less consolidated subcrop, and accumulation of airborne terrestrial dust on the surface and the connected karstic cavities beneath the surface. The majority of the pores and larger cavities were filled with ostracode-bearing carbonate mud, probably during the next inundation stage when peritidal conditions resumed. This was followed by precipitation of isopachous cement under phreatic conditions. At the same time,

Fig. 11 (continued)



erosion of the relatively elevated areas continued, leading to redeposition of the airborne fines and accumulation of rip-ups of the consolidated, blackened and pedogenically altered sediments in the depressions of the tidal flat or in the tidal channels.

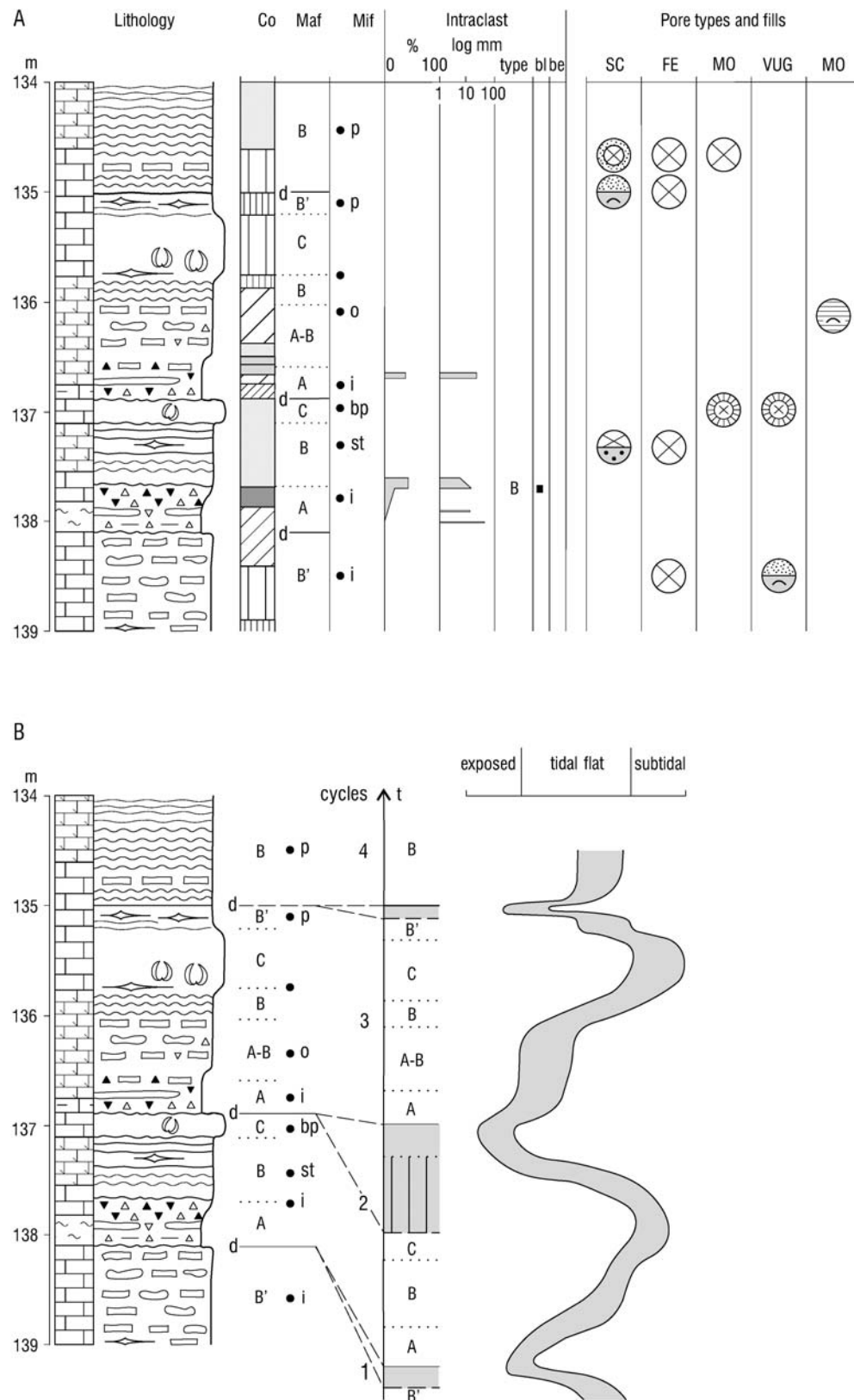
Metre-scale paleokarstic features could be observed at three levels in core Po-89 (see Fig. 6). These are enhanced fissures, sinkholes, or dissolution and collapse cavities (their geometry could not be recognised in core) filled by red marl. Detail of one of these cavities, probably of

collapse origin is shown on Fig. 14F. The larger karstic cavities were probably formed during relatively long subaerial exposure intervals (3rd or 4th order discontinuities; Esteban 1991).

#### *Upper Dachstein Limestone (Rhaetian)*

The features of the peritidal facies described above are based on studies of the Norian Dachstein Limestone in the

**Fig. 12 A** Lithology, macrofacies and microfacies types, intraclasts, pores and pore filling and **B** interpretation of the paleoenvironment in the 134–139-m interval of core Po-89, Bakony Mts.





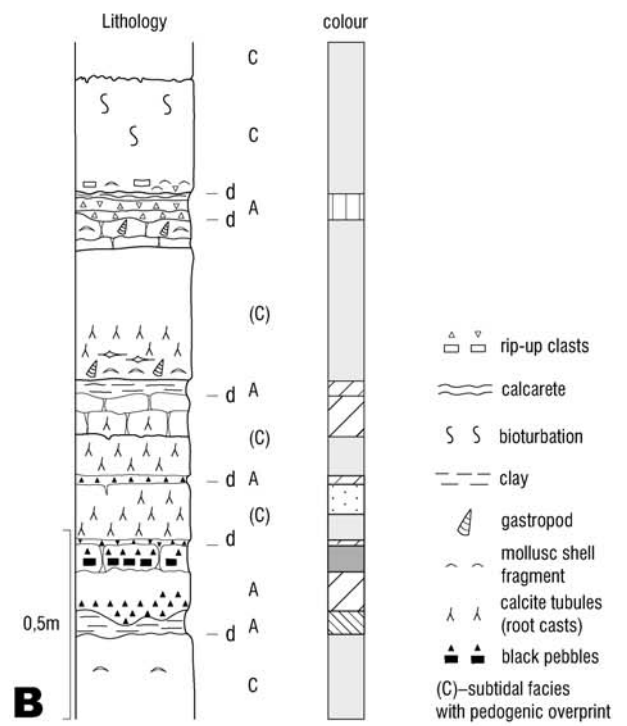
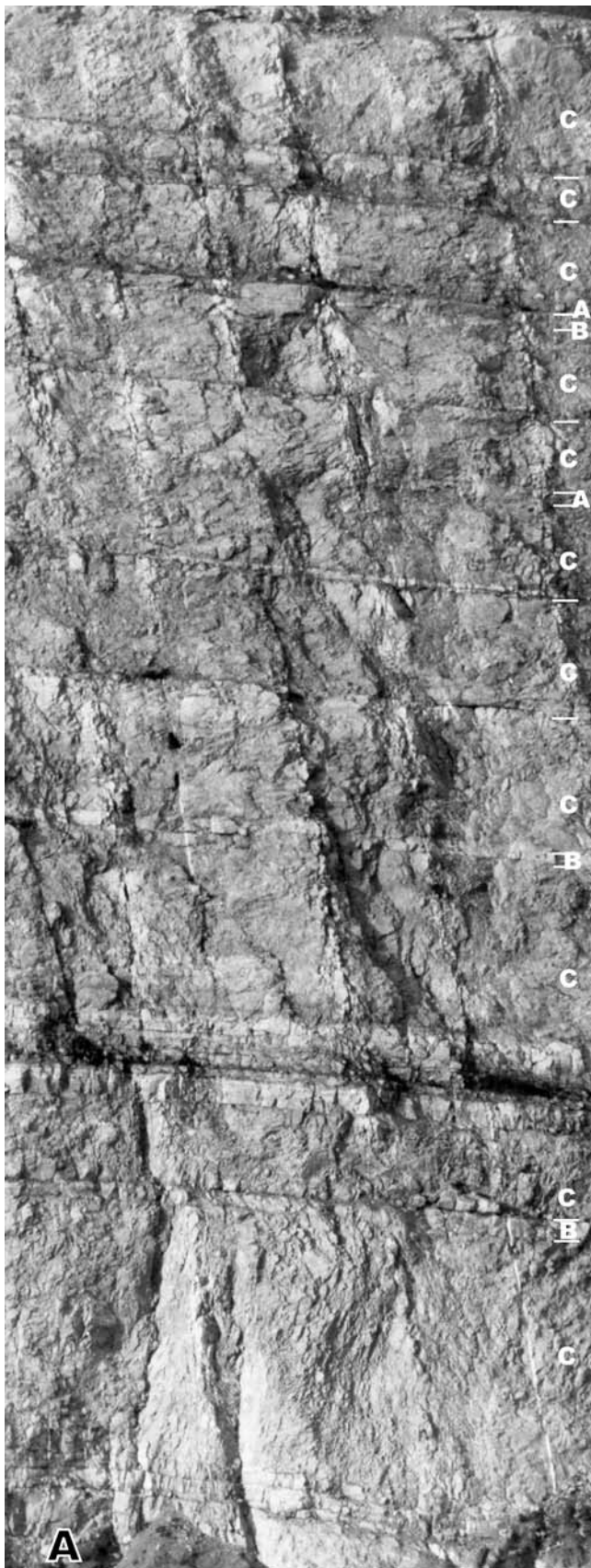
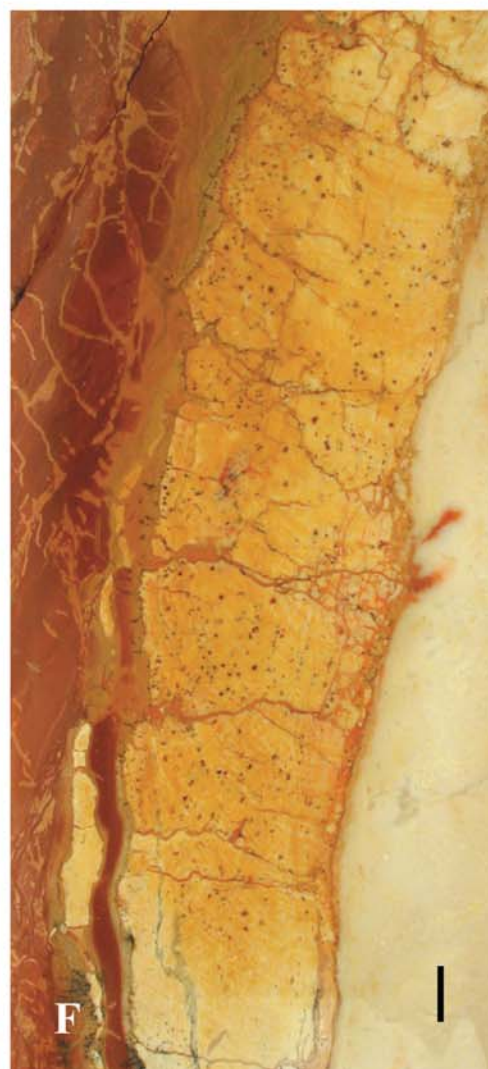
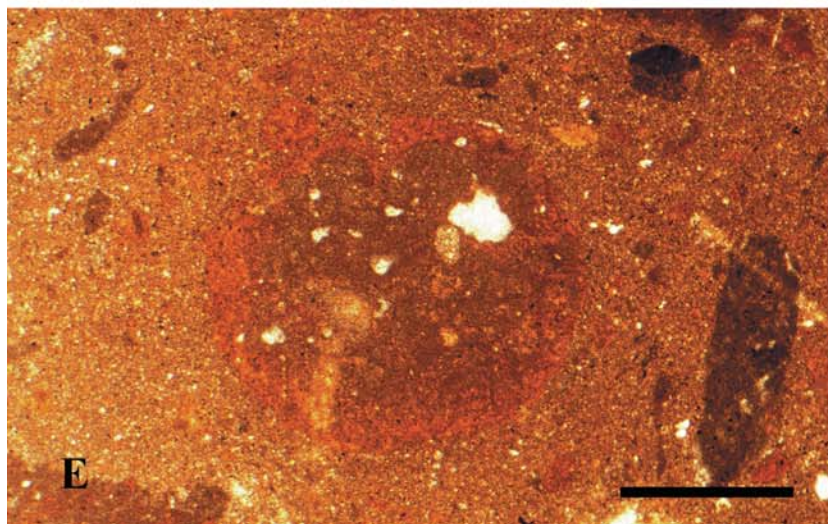
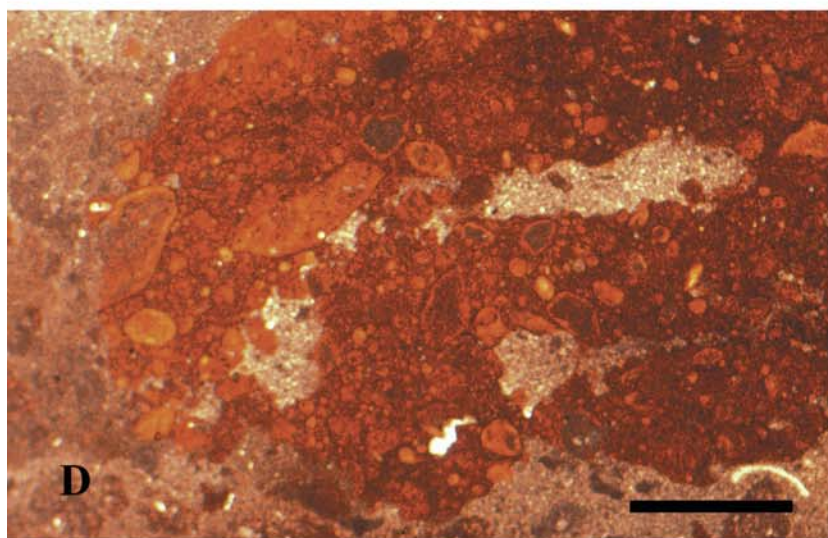
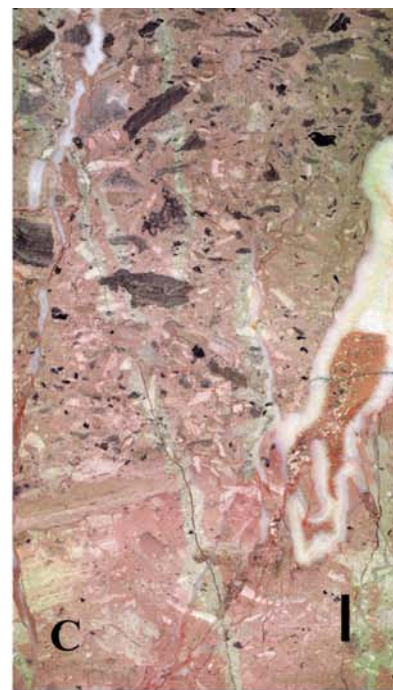


**Fig. 13** **A** Lofer cyclic succession in the upper part of the Dachstein Limestone (Rhaetian) that is punctuated by an anomalously thick peritidal interval marked by a *black bar*. Kecskekő

Quarry, Gerecse Mts. **B** Measured section of the marked interval. For legend of colours (Co) see Fig 7







Northern Bakony Mts. There is no significant difference in character of the peritidal beds neither in the Norian or in the Rhaetian part of the succession between the Northern Bakony and the Gerecse Mts. located about 100 km northeast of the Northern Bakony (Haas 1995a, 1995b). Although the basic facies characteristics of the peritidal beds do not change in the Rhaetian, approximately in the topmost 200 m of the Dachstein Limestone (Haas 1995b), there are remarkable differences in the make-up of the cycles and in the thickness of the peritidal layers. As far as the cycles are concerned, the main difference is that they are typically truncated, i.e. the regressive peritidal layers are generally missing (see Fig. 4). The thickness of the basal peritidal facies is also reduced; rarely does it exceed 10 cm. According to the studies of Mindszenty and Deák (1999) in the Kecskekő quarry, Gerecse Mts. (for location see Fig. 2), the clay in the layers that overlies the microkarstic disconformity surfaces (Member A) is not pedogenic but probably airborne, and the “paleosol” beds are actually inter/supratidal sediments that were affected only by weak pedogenic alteration.

The succession is punctuated by anomalous intervals, 1–2 m thick. Grey or yellowish grey subtidal limestone layers alternate with pinkish or greenish, intraclastic argillaceous limestone layers. An example for this in the Kecskekő quarry is shown on Fig. 13. These intervals can be considered as series of condensed cycles (“minicycles”) reflecting low accommodation. Very shallow inundation of the platform was punctuated by periods of subaerial exposure with incipient pedogenesis of the previously deposited sediments. (Haas 1995b).

Anomalous intervals that were recognisable even in cores, were applied for correlation of bundles of cycles in the Gerecse Mts. Within bundles bounded by anomalous intervals, the majority of the basic cycles could also be recognised in several cores over a distance of about 10 km from the Kecskekő quarry (Haas 1991).

**Fig. 14** Intraclastic argillaceous micrite (A member) and karstic cavity fill. **A** Intraclastic argillaceous micrite. Larger rip-ups of microbial mat and small black pebbles in red micritic matrix. Note the gradual upward transition into the light grey subtidal C facies. Core Po-89, 243.3–243.5 m. Scale bar is 1 cm. **B** Intraclastic argillaceous micrite. Microbial mat rip-ups in red argillaceous micrite matrix Core Po-89, 100.0–100.2 m. Scale bar is 1 cm. **C** Intraclastic argillaceous micrite. Rip-ups of microbial mat, some of them blackened in red argillaceous micrite matrix. Core Po-89, 202.4–202.6 m. Scale bar is 1 cm. **D** Detail of a lump of paleosol origin, made up of tiny globular grains. Voids, filled by fine sediment are probably root moulds. Note ostracode valve at the *right corner* of the photo that belongs to the wackestone matrix. Core Po-89, 149.6 m. Scale bar is 0.5 mm. **E** Globular grain of paleosol origin and blackened intraclasts in micritic matrix. Core Po-89, 349.6 m. Scale bar is 0.5 mm. **F** Detail of a karstic cavity filled by various sediments. Limestone of subtidal facies (C member) is visible in the *right corner*. It is covered by a yellow limestone layer containing a number of desiccation cracks. Collaps of a karstic cavity may have led to tilting of the bedrock that was followed by filling of the cavity with red marl. Core Po-89, 433.6–433.9 m. Scale bar is 1 cm

## Depositional model for the intervals of emergence

The reconstruction of paleogeographic setting and environmental conditions in the inner part of the Dachstein-type platform of the TR were based mainly on the following considerations:

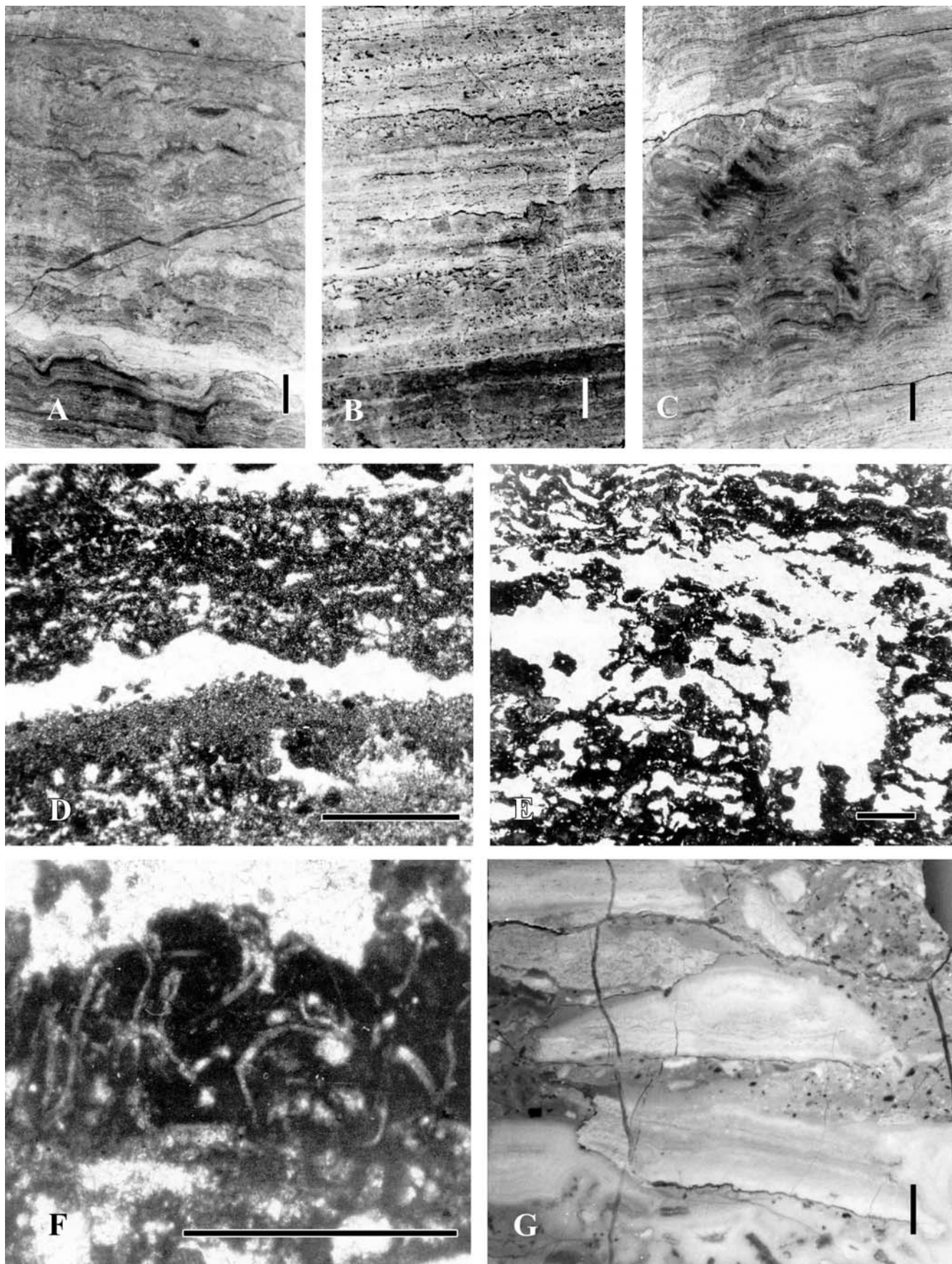
- The large-scale facies distribution (relationships of the lithofacies units)
- The vertical facies succession within the cycles, reflecting the small-scale lateral facies distribution
- Imperfection of the cycles (missing members, truncation)
- The facies characteristics of the peritidal deposits
- The characteristics of the redeposited fines and clasts
- The pore filling materials

For the reconstruction of the depositional environments, the anatomy of modern tidal flats (Shinn 1983; Hardie and Shinn 1986) was also considered, but keeping in mind the significant difference in the dimensions of the relatively narrow modern tidal-flats and the huge Dachstein platform system. The fairly regular alternation of the transgression–regression depositional cycles and the regularity in the facies succession, supported by the results of the Markov chain analyses (Haas 1994), suggest a very gently deepening ramp-like topography. This physiographic setting allowed the development of definite facies belts, although shallow depressions and tidal channels made the actual pattern much more complicated.

A depositional model depicting three critical stages of the cyclic evolution of the platform is presented in Fig. 17. They are as follows:

1. Late highstand—rapid progradation of the tidal flat onto the subtidal inner platform reaching the edge of the permanently inundated outer belt of the platform in the north-eastern part of the TR
2. Lowstand—permanent subaerial exposure in large parts of the TR. Significant (dm-scale) erosion, microkarstification at the surface, development of solution cavities (mainly at the water table), accumulation of windblown fines, weak pedogenic alteration, formation of rip-ups, development of regolith veneer, redeposition of the fines and clasts in local depressions.
3. Transgression—re-establishment of the tidal flat above the karstified erosional surface: mixing of carbonate mud, wind-blown fines, and lag sediments in the depressions and tidal channels, filling of the solution pores and cavities (mainly with carbonate mud of tidal flat pond origin and subsequently with marine calcite cement)





## Discussion

Sander (1936), who first recognised the cyclic nature of the Dachstein Limestone in the Northern Calcareous Alps, attributed the cyclicity to sea-level changes and proposed orbital forcing (21,000-year-equinoxial cycles). Fischer (1964), analysing the options of the tectonic and eustatic controls inclined to favour the eustatic one. Later on Fischer (1975, 1991), Haas (1982, 1991, 1994), Schwarzacher and Haas (1986), Balog et al. (1997), and Cozzi et al. (2003) suggested Milankovitch-driven climatic changes and related sea level changes as the main controlling factors of the Lofer cyclicity.

Goldhammer et al. (1990) studied both Norian Dolomia Principale in the Southern Alps and the Dachstein Limestone at Steinernes Meer in the Northern Calcareous Alps. Within the former, they recognised condensed megacycles consisting of thinning-upward bundles, suggesting Milankovitch-type orbital forcing. In the measured section of the Dachstein Limestone, they observed exclusively shallowing-upward elementary cycles, many with soil caps, and found little evidence of Milankovitch forcing. They concluded that “the Lofer facies deposition was in large measure controlled by short-term variations in the subsidence rate, leading to chaotic stratigraphic distribution of cycle thickness and diagenetic features” and “complex stratigraphies (...) probably record the nonrhythmic sum of pulses of subsidence, sedimentation, autocyclicity, and sea-level variation.” (pp 554–555)

In the last decade, a number of arguments have emerged against orbital forcing and the allocyclic nature of the Lofer cyclicity. Based on the study of the classic area at the Steinernes Meer, in the Northern Calcareous Alps, Satterley and Brandner (1995) came to the conclusion that the Lofer cycles are aperiodic, as is reflected in their exponential thickness-frequency distribution. Satterley (1996) questioned the applicability of the orbital forcing theory for explaining the Lofer cyclicity. He stressed that unambiguous evidence for the predicted hierarchy of the higher and lower frequency cycles are missing. In addition, with the probable lack of an ice cap in the Triassic, glacio-eustasy cannot be invoked. Instead he suggested an autocyclic peritidal depositional model and a role for fault-related tectonic activity.

Enos and Samankassou (1998) measured 139 m of Dachstein Limestone at the Steinernes Meer (Austria) in the neighbourhood of Fischer's and Goldhammer et al.'s measured section, in order to determine the basic pattern of the Lofer cycles. They focused on Member A because this facies is crucial for interpretation of the depth vector of Lofer cycles (shoaling or deepening-upward), since Fischer placed the boundary of the cycle at the base of Member A. In the studied interval, they found neither a real Member A (i.e. no paleosols) nor true unconformities, so they concluded that the sequence is made up of an alternation of B and C members, and is thus rhythmic rather than truly cyclic. Their study on the lateral continuity of the beds (Enos and Samankassou 2002) led to the result that a remarkable proportion of the beds disappears (22%) or shows a significant variation in thickness (11%) laterally. Based on these observations, they reinforced Satterley's conclusion that autocyclic processes may have played a major role in the deposition of the Lofer cycles.

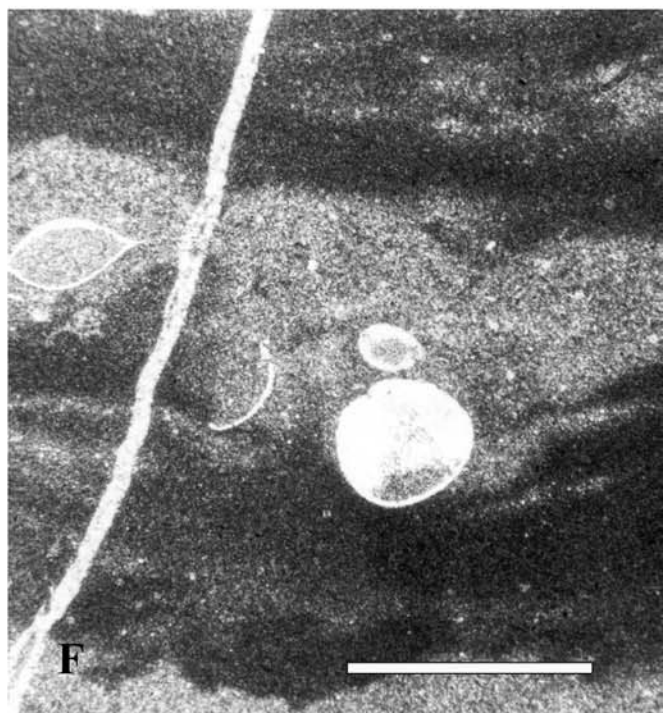
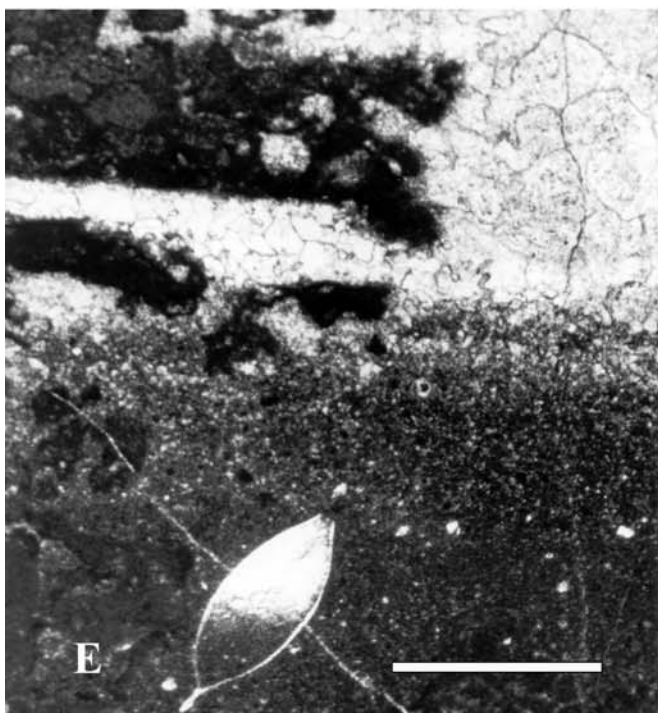
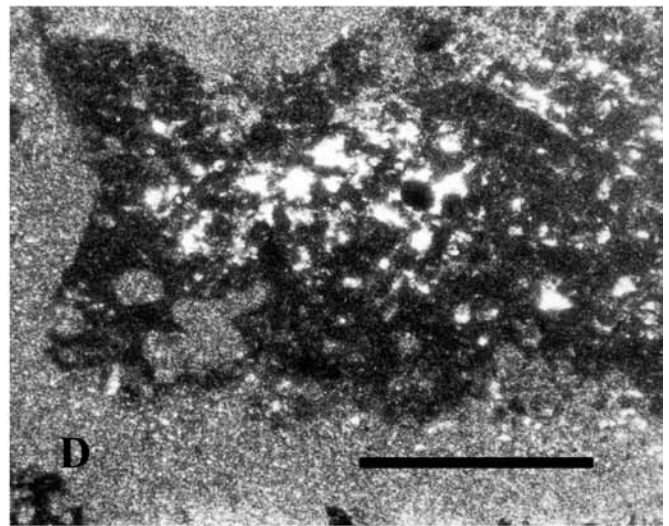
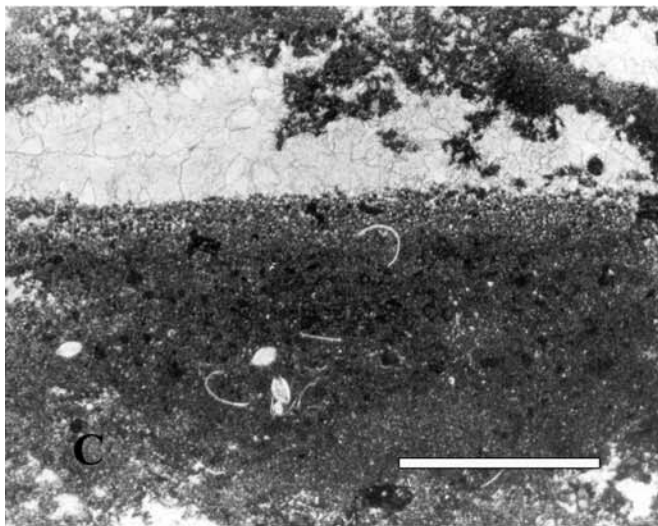
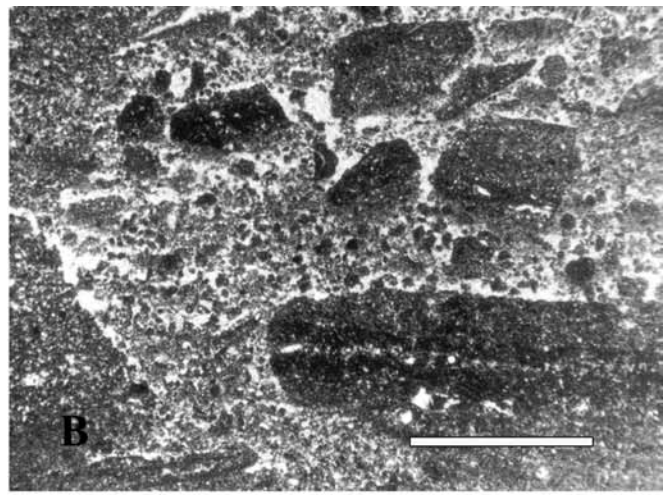
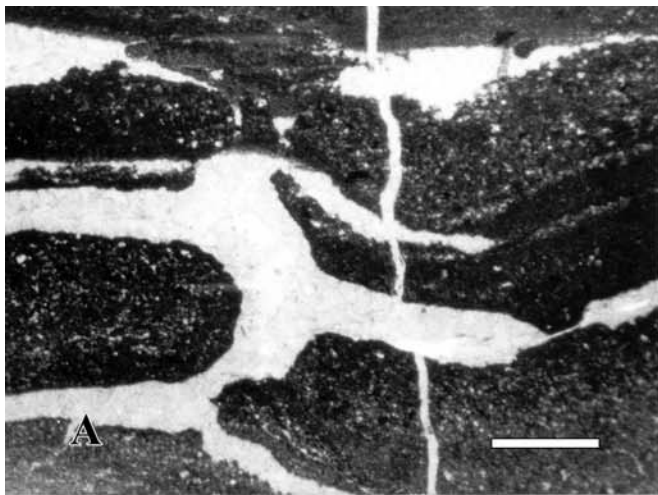
Our previous studies in the TR (Balog et al. 1997) revealed that, although the Milankovitch signal is present, it is highly imperfect due to numerous “missed beats”. It is reflected on the Fischer plots and spectra of time series, showing ratios less than the ideal 5:1 and 20:1 in the cycle bundles expected for 100 and 400-ky-cycles, respectively. As was discussed above, truncated and incomplete cycles are common in the record. It is therefore not surprising that complete cycles are also missing due to non-deposition or erosion, and this is manifested in the imperfection of the stacking pattern of the bundles. However, this does not mean that the Lofer cycles are purely autocyclic. As it was clearly formulated by Sander (1936) and, following his concept, by Schwarzacher (1975:288): “...the absence of cyclicity in the stratigraphic record does not indicate the absence of time cyclicity”.

Strasser (1991) summarised criteria for distinguishing between autocyclic and allocyclic lagoonal–peritidal successions. Both autocyclic and allocyclic cycles display a shallowing-upward trend up to supratidal facies. Local erosion is also compatible with the autocyclicity. In contrast, widespread erosion and intertidal, supratidal or terrestrial overprinting of subtidal facies indicate sea level drop, reflecting allocyclicity. Well-developed cycle boundaries and pervasive cementation and diagenesis suggest long-time emersion, an argument for allocyclicity. The other important point supporting the allocyclic nature of the succession is long distance correlatability of individual cycles. Considering these criteria, the following characteristics of the Lofer cyclic Dachstein-type platform carbonates in the TR appear to be relevant.

The truncation of a significant proportion of the cycles, even parts of the subtidal member, indicates remarkable erosion that was preceded by pervasive cementation and diagenesis of the previously deposited carbonate mud. Under the semi-arid conditions prevailing during the early stage of the platform evolution, tidal flat dolomitisation played an active role in lithification (Balog et al. 1999; Haas and Demény 2002) and dolocretes (terrestrial stromatolites; Wright 1989, 1994) formed on the emerged

**Fig. 15** Microbial stromatolites (B member) **A** Crinkled microbial stromatolite. Core Po-89, 392.6–392.8 m. Scale bar is 1 cm. **B** Microbial stromatolite, flat lamination, bedding-parallel strips of fenestral pores. Core Po-89 476.0–476.3 m. Scale bar is 1 cm. **C** Crinkled microbial stromatolite. Core Po-89, 323.7–323.8 m. Scale bar is 1 cm. **D** Fenestral pores and bedding-parallel cracks (amalgamated pores) in peloidal microbial stromatolite. Core Po-89, 204.7 m. Scale bar is 0.5 mm. **E** Fenestral pores and amalgamated pores in slightly crinkled microbial stromatolite. Core Po-89, 149.9 m. Scale bar is 1 mm. **F** Filaments, probably remnants of calcified cyanobacteria in microbial stromatolite. Core Po-89, 137.3 m. Scale bar is 0.5 mm. **G** Stromatolite intrabreccia. Rudite-sized flat pebbles of microbial mat origin and tiny, commonly blackened intraclasts. Core Po-89, 201.9 m. Scale bar is 1 cm







surface (Balog et al. 1997, 1999). Sub-humid conditions during the later stages of platform evolution (Iannace and Frisia 1994; Balog et al. 1999; Haas 2002) led to irregular erosional surfaces and the development of typical small-scale but rarely metre-scale karstification. Lens-shaped solution cavities formed beneath the surface at the water table. The reddish or greenish clayey horizon above the disconformities indicates accumulation of aerosols due to increased vegetation (Wright 1994). The blackened pebbles also indicate subaerial exposure (Strasser and Davaud 1983; Shinn and Lidz 1983; Vera and Jiménez de Cisneros 1993). It is not surprising that in-situ-preserved terrestrial deposits (paleosols) are rare, since erosion during the next flooding period as a rule led to the demolition of the primary structures and redeposition of the terrestrial sediments.

As far as the correlatability of the cycles is concerned there is no doubt that in the huge quarry at Lábatlan (Gerecse Mts.) the cycles of the Rhaetian Dachstein Limestone can be physically followed without any significant change in their thickness over a distance of about 200 m. Based on exploratory cores, the anomalous intervals (minicycles of pedogenic overprint) could be reliably correlate over a distance of 10 km. Correlation of the basic cycles between the anomalous intervals was also feasible, however less reliable. The arguments discussed above appear to support the allocyclic model, i.e. eustatic control of cyclicity.

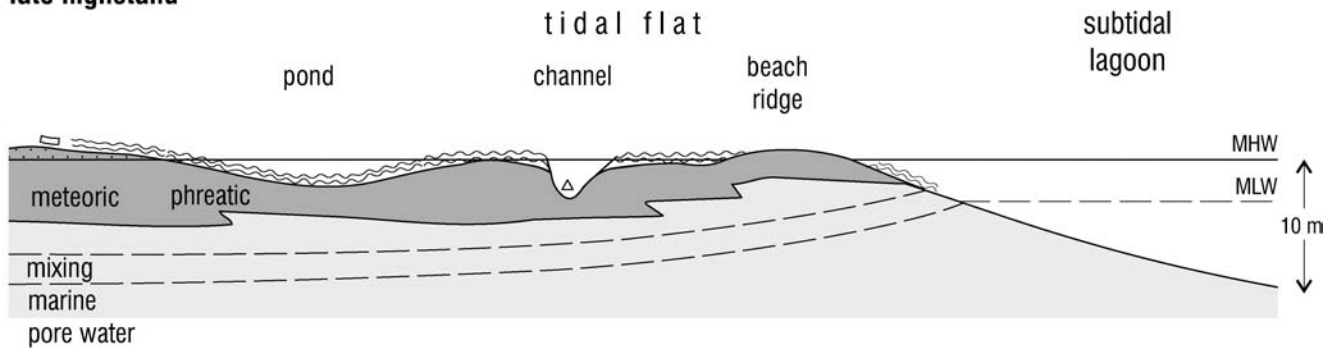
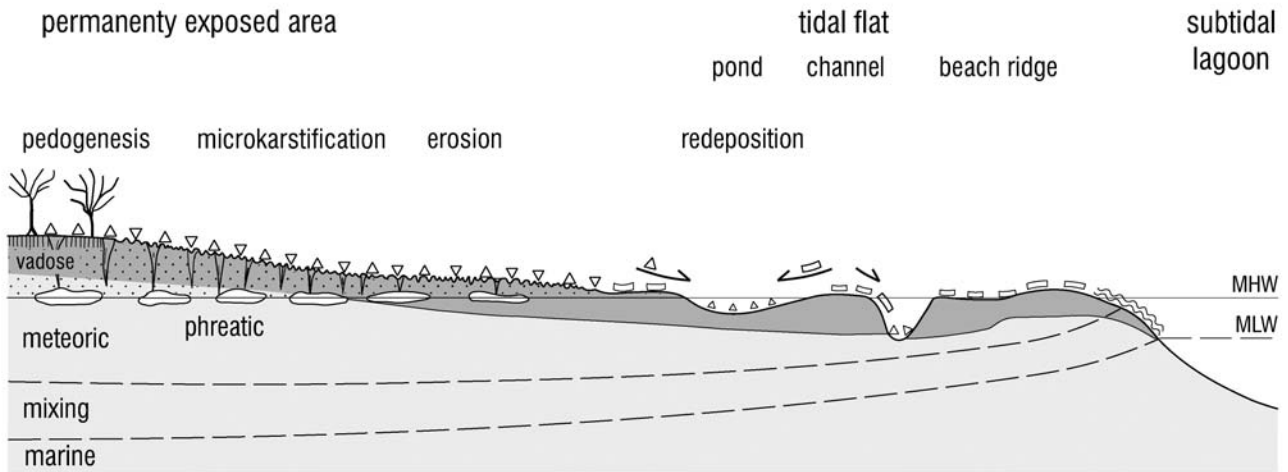
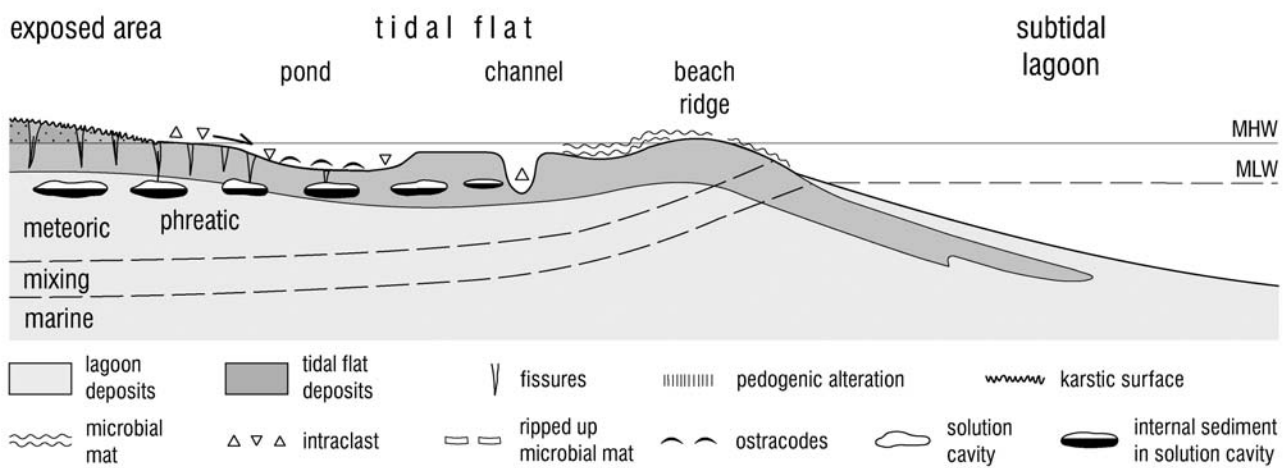
## Conclusions

1. In the Lofer cyclic successions of the Dachstein-type platform carbonates in the Transdanubian Range, the peritidal–subtidal (lagoonal) cycles are typically

bounded by well-developed disconformity surfaces. Uninterrupted alternation of peritidal and subtidal facies also occurs, but rarely.

2. Previous studies of the completely and partially dolomitised sequences and detailed study of the most characteristic intervals of the non-dolomitised Dachstein Limestone suggest that the cycle-bounding disconformities are subaerial erosional surfaces. Truncation of the cycles was preceded by pervasive cementation.
3. In the early stage of platform evolution, during the latest Carnian–Mid-Norian interval, under semi-arid climatic conditions, early tidal-flat dolomitisation led to consolidation of the previously deposited sediment that was accompanied by erosion. The truncation surfaces were commonly covered by dolocretes. During the more humid Late Norian–Rhaetian period, the early cementation was followed by surface and shallow subsurface karstification, accumulation of wind blown dust and pedogenesis. Based on the position of the lens-shaped solution cavities, the paleosurface may have been a few metres above sea-level during low-stands. The fairly regular facies stacking of the cycles suggests an extremely low-angle ramp topography probably with local shoals.
4. The features listed above indicate regularly recurring subaerial exposure conditions that were accompanied by significant erosion. This suggests eustatic control of the cyclicity and justifies the application of allocyclic models. Since the preservation potential of the cycles is far from perfect, and in some cases the sea level may not have reached the level of the platform, the record is frequently imperfect and consequently the bundles do not reflect the ideal Milankovitch patterns.

**Fig. 16** Stromatolite intrabreccia and ostracodal facies. **A** Shrinkage cracks, incipient brecciation in peloidal microbial stromatolite. Core Po-89, 147.2 m. Scale bar is 1 mm. **B** Stromatolite intrabreccia. Rip-ups of peloidal microbial stromatolite. Core Po-89, 147.2 m. Scale bar is 1 mm. **C** Ostracodal, peloidal wackestone internal sediment in the basal part of a lens-shaped solution cavity. Core Po-89, 146.8 m. Scale bar is 1 mm. **D** Rip-ups of peloidal stromatolite origin in a microsparitic matrix. Core Po-89, 148.1 m. Scale bar is 1 mm. **E** Ostracodal, peloidal wackestone internal sediment in the basal part of a lens-shaped solution cavity. Note parallel geopetal fills in the cavity and the ostracode, respectively. Core Po-89, 202.0 m. Scale bar is 0.5 mm. **F** Ostracode remnants in red, argillaceous micrite, microsparite. Core Po-89, 136.2 m. Scale bar is 0.5 mm

**late highstand****lowstand****transgression**

MHW—mean high water; MLW—mean low water

**Fig. 17** Depositional model for the late highstand (tidal flat progradation), lowstand (minimum inundation) and early transgression (lag stage)

**Acknowledgements** This work was supported by the Hungarian Academy of Sciences and the Hungarian Scientific Research Fund (OTKA T037966). I am much obliged to Professor Paul Enos and Professor Werner Piller for their careful and constructive reviews.

## References

- Balog A, Haas J, Read JF, Coruh C (1997) Shallow marine record of orbitally forced cyclicity in a Late Triassic carbonate platform, Hungary. *J Sediment Res* 67(4):661–675
- Balog A, Read JF, Haas J (1999) Climate-controlled early dolomite, Late Triassic cyclic platform carbonates, Hungary. *J Sediment Res* 69(1):267–282
- Benson RH (1959) Ecology of recent ostracodes of the Todos Santos Bay Region, Baja, California, Mexico. *Univ Kansas Paleontol Contrib Arthropoda Art* 1:1–80
- Bossellini A (1967) La tematica deposizionale della Dolomia Principale (Dolomiti e Prealpi Venete). *Boll Soc Geol It* 86:133–167
- Bosellini A, Hardie LA (1988) Facies e cicli della Dolomia Principale delle Alpi Venete. *Mem Soc Geol It* 30:245–266
- Choquette PW, James NP (1988) Introduction. In: Choquette PW, James NP (eds) *Paleokarst*. Springer, Berlin Heidelberg New York, pp 1–21
- Cozzi A, Hinnov LA, Hardie LA (2003) Facies and cyclostratigraphy of Dachstein Limestone in the Julian Alps (N.E. Italy): new insights on the Lofer Cyclothem controversy. In: Abstracts of the field symposium on Triassic geochronology and cyclostratigraphy. September 2003, St. Christina, Italy, p 33
- Dimitrijevic MN, Dimitrijevic MD (1982) Lofer-facies severnog Zlatibora. 10. Jubilarni Kongres geologa Jugoslavije, Zbornik radova 1:455–471
- Dimitrijevic MN, Dimitrijevic MD (1991) Triassic carbonate platform of the Drina-Ivanica element (Dinarides). *Acta Geol Hung* 34(1–2):15–44
- Enos P, Samankassou E (1998) Lofer cyclothem revisited (late Triassic, Northern Alps, Austria). *Facies* 38:207–228
- Enos P, Samankassou E (2002) Lateral variations in Dachstein Limestone (Triassic, Austria). In: *Abst. of the 16th Int. Sedimentological Congress*. July 2002, Johannesburg, p 88
- Esteban M (1991) Paleokarst: practical application. In: Wright VP, Smart P, Esteban M (eds) *Paleokarst and paleokarst reservoirs*. Occas, Univ Reading, Reading, pp 89–119
- Fischer AG (1964) The Lofer cyclothem of the Alpine Triassic. *Kansas Geol Surv Bull* 169:107–149
- Fischer AG (1975) Tidal deposits, Dachstein Limestone of the North-Alpine Triassic. In: Ginsburg RN (ed) *Tidal deposits: a casebook of recent examples and fossil counterparts*. Springer, Berlin Heidelberg New York, pp 234–242
- Fischer AG (1991) Orbital cyclicity in Mesozoic strata. In: Einsele G, Ricken W, Seilacher A (eds) *Cycles and events in stratigraphy*. Springer, Berlin Heidelberg New York, pp 48–62
- Foos AM (1991) Aluminous lateritic soils, Eleuthera, Bahamas: a modern analog to carbonate paleosols. *J Sediment Petrol* 61:340–348
- Friedman GM, Amiel AJ, Braun M, Miller DS (1973) Generation of carbonate particles and laminites in algal mats: example from sea-marginal hypersaline pool, Gulf of Aquaba, Red Sea. *Bull Am Assoc Petrol Geol* 57:541–557
- Fruth I, Scherreihs R (1984) Hauptdolomit: sedimentary and paleogeographic models (Norian, Northern Calcareous Alps). *Geol Rundsch* 73:305–319
- Fülöp J (1976) The Mesozoic basement horst blocks of Tata. *Geol Hung Ser Geol* 16:1–122
- Gawlick H-J (2000) Paleogeographie der Ober-Trias Karbonatplattform in den Nördlichen Kalkalpen. *Mitt Ges Geol Bergbaustud Österr* 44:45–95
- Gawlick H-J, Krystin L, Lein R, Mandl GW (1999) Tectonostratigraphic concept for the Juvavic domain. *Tübinger Geowiss Arbeiten A* 52:95–99
- Gecse ÉT (1984) Cyclic Upper Triassic formations in the neighbourhood of Fenyőfő, Csesznek, Bakonyoszlop, Dudar and Súr (in Hungarian, English summary). Annual report, Hungarian Geol Inst, Budapest, pp 317–335
- Ginsburg RN (1971) Landward movement of carbonate mud: new model for regressive cycles in carbonates (abs). *Bull Am Assoc Petrol Geol* 55:340–341
- Ginsburg RN, Hardie LA (1975) Tidal and storm deposits, north-western Andros Island, Bahamas. In: Ginsburg RN (ed) *Tidal deposits: a casebook of recent examples and fossil counterparts*, vol 8. Springer, Berlin Heidelberg New York, pp 201–208
- Goldhammer RK, Dunn PA, Hardie LA (1990) Depositional cycles, composite sea-level changes, cycle stacking patterns, and the hierarchy of stratigraphic forcing: examples from Alpine Triassic platform carbonates. *Geol Soc Am Bull* 102:535–562
- Gradstein F, Ogg J (1996) A Phanerozoic time scale. *Episodes* 19:3–6
- Gümbel CW (1857) Untersuchungen in den Bayerischen Alpen zwischen der Iser und Salzach. *Jb Geol R A* 8:146–151
- Haas J (1982) Facies analysis of the cyclic Dachstein Limestone Formation (Upper Triassic) in the Bakony Mountains, Hungary. *Facies* 6:75–84
- Haas J (1991) A basic model for Lofer cycles. In: Einsele G, Ricken W, Seilacher A (eds) *Cycles and events in stratigraphy*. Springer, Berlin Heidelberg New York, pp 722–732
- Haas J (1994) Lofer cycles of the Upper Triassic Dachstein platform in the Transdanubian Mid-Mountains (Hungary). *Int. Assoc. Sedimentol., Spec Publ no. 19*, pp 303–322
- Haas J (1995a) Upper Triassic platform carbonates in the Northern Bakony Mts. (in Hungarian, English summary). *Földt Közl* 125:27–64
- Haas J (1995b) Upper Triassic platform carbonates in the Northern Gerecse Mts. (in Hungarian, English summary). *Földt Közl* 125:259–293
- Haas J (2002) Origin and evolution of Late Triassic platform carbonates in the Transdanubian Range (Hungary). *Geol Carp* 53:159–178
- Haas J, Balog A (1995) Facies characteristics of the Lofer cycles in the Upper Triassic platform carbonates of the Transdanubian Range, Hungary. *Acta Geol Hung* 38(1):1–36
- Haas J, Budai T (1995) Upper Permian-Triassic facies zones in the Transdanubian Range. *Riv It Paleontol Stratigr* 101:249–266
- Haas J, Demény A (2002) Early dolomitisation of Late Triassic platform carbonates in the Transdanubian Range (Hungary). *Sediment Geol* 150:225–242
- Haas J, Kovács S, Krystyn L, Lein R (1995) Significance of Late Permian-Triassic facies zones in terrane reconstructions in the Alpine-North Pannonian domain. *Tectonophysics* 242:19–40
- Haas J, Skourtsis-Coroneou V (1995) The Upper Triassic platform sequences in the Transdanubian Range and the Pelagonian Zone s.l.: a correlation. *Geol Soc Greece, Athens, Spec. Publ. no. 4*, pp 195–200
- Hardie LA, Shinn EA (1986) Carbonate depositional environments, modern and ancient, Tidal flats. *Colorado School Mines Q* 81:1–74
- Iannace A, Frisia S (1994) Changing dolomitisation styles from Norian to Rhaetian in the southern Tethys realm. In: Purser B, Tuckes M, Zenger D (eds) *Dolomites*. IAS, Blackwell, Oxford, Spec. Publ. no. 21, pp 55–74
- Jadoul F, Berra F, Frisia S (1992) Stratigraphic and paleontologic evolution of a carbonate platform in an extensional tectonic regime: example of the Dolomia Principale in Lombardy (Italy). *Rev It Paleontol Stratigr* 91:479–511
- James NP (1972) Holocene and Pleistocene calcareous crusts (caliche) profiles: criteria for subaerial exposure. *J Sediment Petrol* 42:817–836
- Mandl GW (2000) The Alpine sector of the Tethyan shelf: examples of Triassic to Jurassic sedimentation and deformation from the Northern Calcareous Alps. *Mitt Österr Geol Ges* 92:61–77
- Michalik J (1980) A paleoenvironmental and paleoecological analysis of the Western Carpathian part of the northern Tethyan

- nearshore region in the latest Triassic time. *Riv It Paleontol Stratigr* 85:1047–1064
- Michalik J (1993) Mesozoic tensional basins in the Alpine-Carpathian Shelf. *Acta Geol Hung* 36(4):395–403
- Mindszenty A, Deák J (1999) Carbonate paleosols from the Upper Triassic of the Gerecse mountains, Hungary (in Hungarian, English summary). *Földt Közl* 129(2):213–248
- Monty CL, Hardie LA (1976) The geological significance of freshwater blue-green algal calcareous marsh. In: Walter MR (ed) *Stromatolites*. Elsevier, Amsterdam, pp 447–477
- Ogorelec B, Buser S (1996) Dachstein Limestone from Krn in Julian Alps (Slovenia). *Geologija* 39:133–155
- Ogorelec B, Rothe P (1992) Mikrofacies, Diagenese und Geochemie des Dachsteinkalkes und Hauptdolomits in Süd-West-Slowenien. *Geologija* 35:81–18
- Oravecz J (1963) Questions stratigraphiques at facies des formations triasiques supérieures de la montagne Centrale de Transdanubie (in Hungarian, French summary). *Föld Közl* 93/2:63–67
- Oravecz-Scheffer A (1987) Triassic foraminifers of the Transdanubian Central Range. *Geol Hung Ser Pal* 50:1–331
- Peters KF (1855) Bericht über die geologische Aufnahme in Karnten. *Jb Geol R A* 6:508–580
- Pia J (1923) Geologische Skizze des Steinernes Meeres bei Saalfelden mit besonderer Rücksicht auf die Dioporensteine. *Sitz Ber Österr Akad Wiss Math Naturw* 132:35–79
- Piller W (1976) Facies und Lithostratigraphie des gebankten Dachsteinkalkes (Obertrias) am Nordrand des Toten Gebirges (S Grünau/Almtal, Oberösterreich). *Mitt Ges Geol Bergbaustud Öster* 23:133–152
- Pomoni-Papaioannou F, Trifonova E, Tsaila-Monopolis S, Katsavrias N (1986) Lofer type cyclothems in a Late Triassic dolomitic sequence on the eastern part of the Olympus. *Inst Geol Min Exp., Athens*, pp 403–417
- Read JF (1974) Calcrete deposits and Quarternary sediments, Edel Province, Western Australia. In: Logan BW, Read JF, Hagan GM, Hoffman P, Brown RG, Woods PJ, Gebelin CD (eds) *Evolution and diagenesis of Quarternary carbonate sequences, Shark Bay, Western Australia*. AAPG Mem 22:250–282
- Read JF, Horbury AD (1993) Eustatic and tectonic controls on porosity evolution beneath sequence-bounding unconformities and parasequence disconformities on carbonate platforms. In: Horbury AD, Robinson AG (eds) *Diagenesis and basin development*. AAPG Stud Geology 36:155–197
- Riding R (1991) Classification of microbial carbonates. In: *Calcareous algae and stromatolites*. Springer, Berlin Heidelberg New York, pp 21–51
- Sander B (1936) Beiträge zur Kenntnis der Anlagerungsgefüge. *Miner Petr Mitt* 48: 27–139
- Satterley AK (1996) The interpretation of cyclic succession of the Middle and Upper Triassic of the Northern and Southern Alps. *Earth Sci Rev* 40:181–207
- Satterley AK, Brandner R (1995) The genesis of Lofer cycles of the Dachstein Limestone, Northern Calcareous Alps, Austria. *Geol Rundsch* 84:287–292
- Schwarzacher W (1948) Über die sedimentäre Rhythmik des Dachsteinkalkes von Lofer. *Geol B A Verh* 10–12:175–18
- Schwarzacher W (1954) Die Grossrhythmik des Dachsteinkalkes von Lofer. *Tschermaks Min Petr Mitt* 4:44–54
- Schwarzacher W (1975) Sedimentation models and quantitative stratigraphy. In: *Developments of sedimentology*, vol 19, Elsevier, New York, 382 pp
- Schwarzacher W, Haas J (1986) Comparative statistical analysis of some Hungarian and Austrian Upper Triassic peritidal carbonate sequences. *Acta Geol Hung* 29:175–196
- Shinn EA (1983) Tidal flat environment. In: Sholle PA, Bebout DG, Moore CH (eds) *Carbonate depositional environments*. Mem Amer Assoc Petrol Geol 33:173–210
- Shinn EA, Lidz B (1983) Blackened limestone pebbles: fire at subaerial unconformities. In: Jammes NP, Choquette PW (eds) *Paleokarst*. Springer, Berlin Heidelberg New York, pp 117–131
- Simony F (1847) Winteraufenthalt im Hallstätter Schneegebirge und 3. Ersteigung der hohen Dachsteinspitze. *Ber Mitt Freund Naturw* 2:207–221
- Strasser A (1984) Black-pebble occurrence and genesis in Holocene carbonate sediments (Florida Keys, Bahamas, and Tunisia). *J Sediment Petrol* 54:1097–1109
- Strasser A (1991) Lagoonal-peritidal sequences in carbonate environments: autocyclic and allocyclic processes. In: Einsele G, Ricken W, Seilacher A (eds) *Cycles and events in stratigraphy*. Springer, Berlin Heidelberg New York, pp 709–721
- Strasser A, Davaud E (1983) Black pebbles of the Purbeckian (Swiss and French Jura): lithology, geochemistry and origin. *Ecol Geol Helv* 76:551–580
- Tollmann A (1976) Analyse des klassischen nordalpinen Mesozoicums. *Stratigraphie, Fauna und Facies der Nördlichen Kalkalpen*. Deuticke, Wien 580 pp
- Tollmann A (1985) *Geologie von Österreich, Band 2*. Deuticke, Wien 710 pp
- Tucker ME (1990) Modern carbonate environments. In: Tucker ME, Wright VP (ed) *Carbonate sedimentology*. Blackwell, Oxford, pp 70–100
- Végh-Neubrant E (1957) Sedimentpetrographische Eigenschaften karbonatischer Gesteine aus dem ungarischen Trias (in Hungarian, German summary). *Földt Közl* 87/1:19–25
- Végh-Neubrant E (1960) Petrologische Untersuchung der Obertrias-Bildungen der Gerecsegebirges in Ungarn. *Geol Hung Ser Geol* 12:1–130
- Végh-Neubrant E (1982) Triasische Megalodontaceae: Entwicklung, Stratigraphie und Paleontologie. *Akadémiai Kiadó, Budapest*, 526 pp
- Vera JA, Jiménez de Cisneros C (1993) Palaeogeographic significance of black pebbles (Lower Cretaceous, Pre-Betic, southern Spain). *Paleogeogr Paleoclimatol Paleoecol* 102:89–102
- Wright VP (1989) Terrestrial stromatolites: a review. *Sediment Geol* 65:1–13
- Wright VP (1994) Paleosols in shallow marine carbonate sequences. *Earth Sci Rev* 35:367–395
- Wright VP, Tucker ME (1991) Calcretes: an introduction. In: Wright VP, Tucker ME (eds) *Calcretes*. IAS Reprint Series, vol 2, Blackwell, Oxford, pp 1–22
- Zankl H (1967) Die Karbonatsedimente der Obertrias in den nördlichen Kalkalpen. *Geol Rundsch* 56:128–139